Journal of Medicinal Chemistry

pubs.acs.org/jmc Article

From a Designer Drug to the Discovery of Selective Cannabinoid Type 2 Receptor Agonists with Favorable Pharmacokinetic Profiles for the Treatment of Systemic Sclerosis

Bei-Er Jiang,[⊥] Xingwu Jiang,[⊥] Qiansen Zhang,[⊥] Qiuwen Liang, Zi-Liang Qiu, Xiang-Bai Sun, Jun-Jie Yang, Si Chen, Chunyang Yi, Xiaolei Chai, Mingyao Liu, Li-Fang Yu,* Weiqiang Lu,* and Han-Kun Zhang*

Cite This: *J. Med. Chem.* 2021, 64, 385−403 Read Online

ACCESS | Metrics & More | Article Recommendations | Supporting Information

ABSTRACT: Synthetic cannabinoids, as exemplified by SDB-001 (**1**), bind to both CB1 and CB2 receptors and exert cannabimimetic effects similar to (−)-*trans*-Δ^9-tetrahydrocannabinol, the main psychoactive component present in the cannabis plant. As CB1 receptor ligands were found to have severe adverse psychiatric effects, increased attention was turned to exploiting the potential therapeutic value of the CB2 receptor. In our efforts to discover novel and selective CB2 receptor agonists, **1** was selected as a starting point for hit molecule identification and a class of 1*H*-pyrazole-3-carboxamide derivatives were thus designed, synthesized, and biologically evaluated. Systematic structure−activity relationship investigations resulted in the identification of the most promising compound **66** as a selective CB2 receptor agonist with favorable pharmacokinetic profiles. Especially, **66** treatment significantly attenuated dermal inflammation and fibrosis in a bleomycin-induced mouse model of systemic sclerosis, supporting that CB2 receptor agonists might serve as potential therapeutics for treating systemic sclerosis.

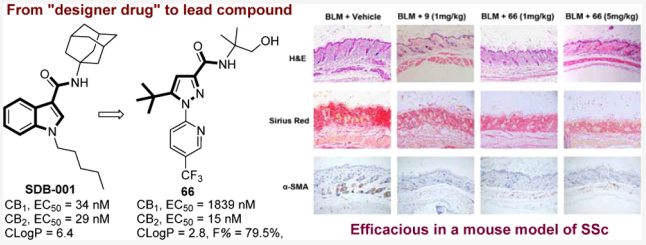

INTRODUCTION

Cannabis sativa has a widespread use for recreational, medical, and religious purposes in many cultures for thousands of years and is the unique source of more than 60 phytocannabinoids.[1] Among these biologically active substances, (−)-*trans*-Δ^9-tetrahydrocannabinol (Δ^9-THC, **2**) is the principal psychoactive component in *C. sativa* and the most studied one (Figure 1). It was originally isolated and elucidated by Mechoulam and his coworkers in 1964, which resulted in the further identification of the endocannabinoid system (ECS).[2−4] The ECS mainly consists of two types of cannabinoid receptors (CB1 and CB2) and a series of endogenous ligands such as anandamide and 2-arachidonoylglycerol, as well as some metabolic enzymes responsible for the biosynthesis and degradation of endocannabinoids.[5]

CB1 and CB2 receptors are both class A rhodopsin-like G-protein-coupled receptors (GPCRs), sharing 44% overall homology and more than 60% homology in the transmembrane domain that encompasses the ligand-binding pocket.[6] The CB1 receptor is widely expressed in the central nervous system (CNS), having a high level particularly in the brain and spinal cord.[7,8] It is a potential target for treating obesity, metabolic syndrome, and several neurodegenerative diseases. However, it is also believed that the stimulation of the CB1 receptor is responsible for several undesirable side effects. Rimonabant (**3**), a selective CB1 receptor blocker originally approved in Europe as an antiobesity agent in 2006, was removed from the market due to its severe adverse psychiatric effects such as anxiety, depression, and suicidal thoughts.[9−11] In contrast, the CB2 receptor is abundant in the peripheral immune system and has much lower expression in the CNS compared to the CB1 receptor.[16] It was found to be heavily implicated in a host of pathophysiological conditions including chronic and neuropathic pain,[12,13] neurodegenerative disorders,[14,15] cancers,[16] osteoporosis,[17] and inflammation-associated pathologies.[18,19] Thus, the development of novel ligands targeting CB2 receptor with high potency and selectivity may hold promise to fulfill multiple unmet clinical needs while avoiding the psychotropic side effects caused by interaction with the CB1 receptor. To date, there are several cannabinoid drugs such as Nabiximols (approved in the United Kingdom), Nabilone (approved in the United States), Cannabidiol (approved in the United States), and Dronabinol (approved in the United States) that have been

Received: June 15, 2020
Published: December 31, 2020

https://dx.doi.org/10.1021/acs.jmedchem.0c01023
J. Med. Chem. 2021, 64, 385−403

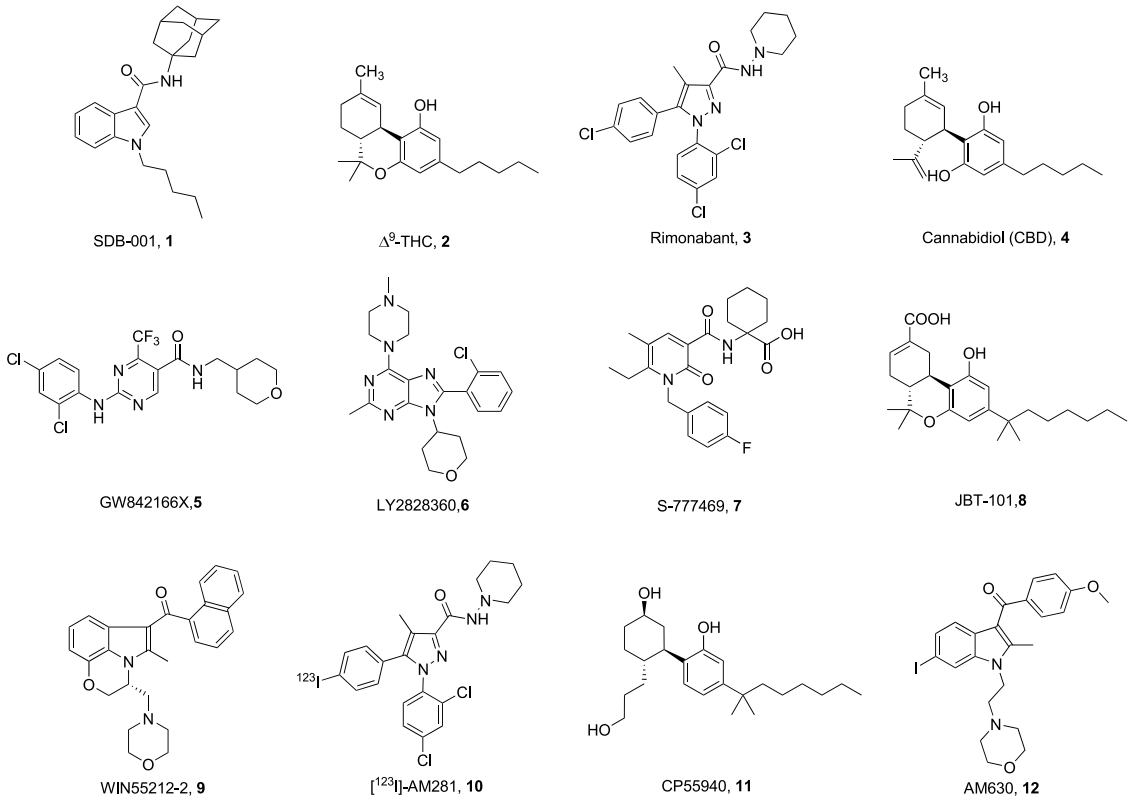

Figure 1. Representative cannabinoid receptor ligands disclosed in the literature.

approved for clinical use, all of which are derived from naturally occurring active constituents (**2** and **4**) of *C. sativa*. On the other hand, as shown in Figure 1, a number of synthetic cannabinoids with a preference for the CB2 receptor are under clinical evaluation mostly in the area of pain management or inflammation-related diseases, such as GW842166X[20] (**5**), LY2828360[21] (**6**), and S-777469[22] (**7**). Among these investigational drugs, ajulemic acid (JBT-101, **8**), an orally active synthetic CB2 agonist, is the most promising one developed by Corbus Pharmaceuticals and has entered phase 3 clinical studies for treating dermatomyositis and systemic sclerosis (SSc).[23]

SSc is a complex autoimmune disease that is characterized by vasculopathy, inflammation, and autoimmunity, which leads to progressive fibrosis in the skin and multiple internal organs.[24,25] It has a worldwide distribution and severely impacts patient quality of life with high morbidity and mortality. SSc is heterogeneous in its clinical presentation, and common treatments such as immunomodulatory drugs and glucocorticoids have limited therapeutic effects and poor prognosis.[26] At present, safe and effective therapeutics that can alleviate or reverse the progression of SSc are urgently needed.[27] Recently, mounting studies have demonstrated that the ECS plays key roles in modulating fibrosis, inflammation, and vasodilatation, all of which are dysregulated in SSc.[28] It was found that CB2 receptor knockout mice ($CB2^{-/-}$ mice) showed increased susceptibility to bleomycin (BLM)-induced dermal fibrosis compared to wild-type mice. In addition, activation of CB2 receptor can exert antifibrotic effects in experimental models of SSc by reducing leukocyte infiltration into skin lesions and preventing tissue damage in pathologic fibrosis.[29] In terms of CB2 receptor ligands, WIN55212−2 (**9**), a nonselective cannabinoid receptor agonist, dramatically reduced the dermal fibrosis and the synthesis of extracellular matrix components in a mouse model of BLM-induced SSc.[30] Compound **8** received orphan drug designation from the FDA as a Fast Track Development Program for the treatment of chronic inflammation and SSc, and is currently in a phase 3 clinical trial.[23,31] Taken together, the evidence suggests that the CB2 receptor might be a potential molecular target for treating SSc.

SDB-001 (**1**) is an indole-based synthetic cannabinoid and was first identified as a designer drug in the illegal market by Japanese researchers from the National Institute of Health Sciences in 2012. It exhibits full agonist activity at both CB1 (EC_{50} = 34 nM, E_{max} = 98%) and CB2 (EC_{50} = 29 nM, E_{max} = 91%) receptors, and has potent cannabimimetic effects in rats.[32] Although its *in vivo* pharmacological activity was similar to that of partial agonist **2**, compound **1** may cause more severe psychiatric complications due to its full agonism and the longer duration of its pharmacologic effects on the CB1 receptor.[33,34] In addition, as the primary psychoactive components in K2/Spice products, derivatives of compound **1** are difficult to detect in standardized drug testing due to their structural diversity.[35] Since then, considerable research efforts have been devoted to unraveling the structure−activity relationships (SARs) of compound **1** and its structural analogues for better understanding the pharmacological mechanism underlying the distinct toxic effects of synthetic cannabinoids compared to compound **1**.[36−41] In most of these studies, the central indole ring of compound **1** was retained, and the SAR studies mainly focused on the substituents at the 1-indole position and in the carboxamide group at the 3-indole position. Recently, a number of studies have indicated that compound **1** and its derivatives were rapidly metabolized when incubated with human hepatocytes or human liver microsomes *in vitro*.[42,43] Therefore, it is not surprising that all of the *in vivo* efficacy studies disclosed in the above-mentioned articles were carried out through

https://dx.doi.org/10.1021/acs.jmedchem.0c01023
J. Med. Chem. 2021, 64, 385−403

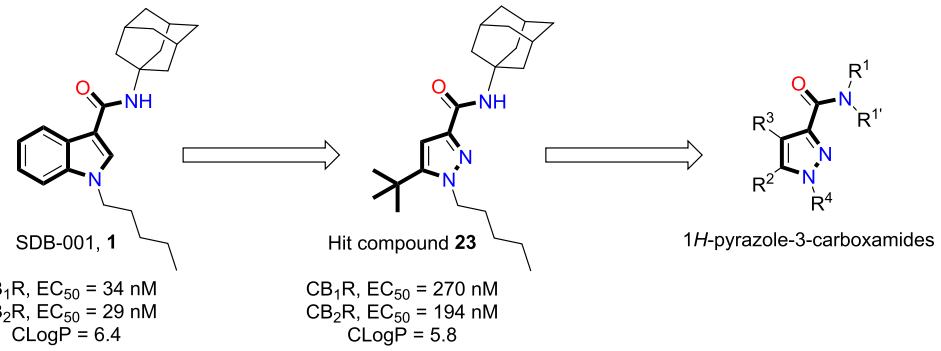

Figure 2. Overview of the design of 1*H*-pyrazole-3-carboxamide derivatives reported in this work.

Scheme 1. Synthesis of Compounds 17−40, 45−52, and 54−68[a]

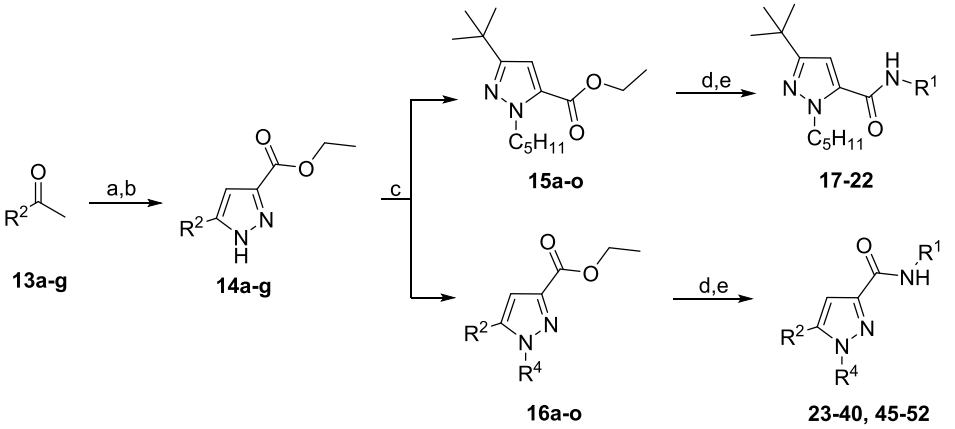

13a-14a R^2 = *t*-Bu
13b-14b R^2 = isopropyl
13c-14c R^2 = neopentyl
13d-14d R^2 = cyclopropyl
13e-14e R^2 = cyclohexyl
13f-14f R^2= trifluoromethyl
13g-14g R^2 = 2,4-DiF-phenyl

15a-16a R^2 = *t*-Bu, R^4 = n-pentyl
15b-16b R^2 = isopropyl, R^4 = n-pentyl
15c-16c R^2 = neopentyl, R^4 = n-pentyl
15d-16d R^2 = cyclopropyl, R^4 = n-pentyl
15e-16e R^2 = cyclohexyl, R^4 = n-pentyl
15f-16f R^2 = trifluoromethyl, R^4 = n-pentyl
15g-16g R^2 = 2,4-DiF-phenyl, R^4 = n-pentyl
15h-16h R^2 = *t*-Bu, R^4 = n-propyl

15i-16i R^2 = *t*-Bu, R^4 = n-butyl
15j-16j R^2 = *t*-Bu, R^4 = n-hexyl
15k-16k R^2 = *t*-Bu, R^4 = 3-F-propyl
15l-16l R^2 = *t*-Bu, R^4 = 4-F-butyl
15m-16m R^2 = *t*-Bu, R^4 = 5-F-pentyl
15n-16n R^2 = *t*-Bu, R^4 = cyclopropylmethyl
15o-16o R^2 = *t*-Bu, R^4 = methoxyethyl

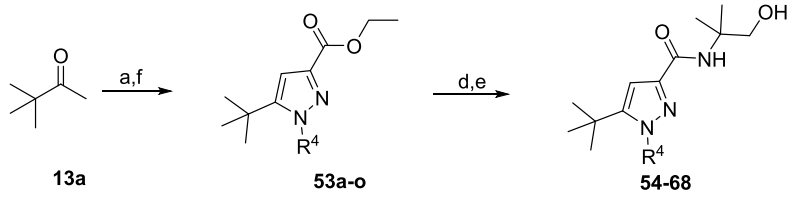

53a R^4 = phenyl
53b R^4 = 4-methylphenyl
53c R^4 = 4-F-phenyl
53d R^4 = 4-Cl-phenyl
53e R^4 = 4-CF_3-phenyl
53f R^4 = 4-methoxypheny
53g R^4 = 4-(trifluoromethoxy)phenyl
53h R^4 = 2,4-difluorophenyl

53i R^4 = 2-pyridyl
53j R^4 = 3-pyridyl
53k R^4 = 2-(5-Cl-pyridyl)
53l R^4 = 2-(5-F-pyridyl)
53m R^4 = 2-(5-CF_3-pyridyl)
53n R^4 = 2-(3-Cl-5-CF_3-pyridyl)
53o R^4 = pyrimidyl

[a]Reagents and conditions: (a) potassium *tert*-butoxide (*t*-BuOK), diethyl oxalate, anhydrous tetrahydrofuran (THF), room temperature (rt), 5 h; (b) $NH_2NH_2{\cdot}H_2O$, acetic acid (AcOH), anhydrous THF, reflux, 3 h, 52−88%; (c) R^4Br, anhydrous THF, reflux, overnight; (d) $LiOH{\cdot}H_2O$, CH_3OH:H_2O:THF = 2:1:2, rt, overnight, 87−98%; (e) R^1NH_2, 2-(7-aza-1*H*-benzotriazole-1-yl)-1,1,3,3-tetramethyluronium hexafluorophosphate (HATU), *N*,*N*-diisopropylethylamine (DIPEA), CH_2Cl_2, rt, 4 h, 65−80%; (f) $R^4NHNH_2{\cdot}HCl$, AcOH, anhydrous THF, reflux, 3 h, 38−76%.

https://dx.doi.org/10.1021/acs.jmedchem.0c01023
J. Med. Chem. 2021, 64, 385−403

Scheme 2. Synthesis of Compounds 41−44[a]

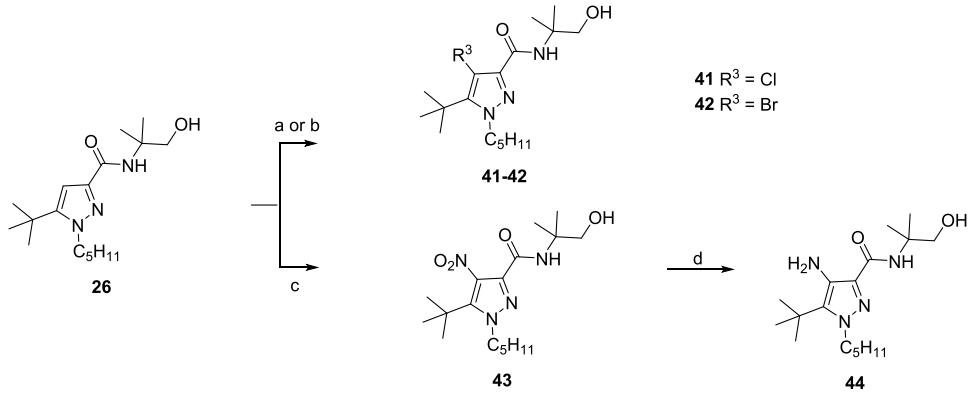

[a]Reagents and conditions: (a) *N*-bromosuccinimide (NBS), dibenzoyl peroxide, chloroform ($CHCl_3$), reflux, overnight, 52%; (b) *N*-chlorosuccinimide (NCS), dibenzoyl peroxide, $CHCl_3$, reflux, overnight, 58%; (c) $Cu(NO_3)_2$, trifluoroacetic anhydride (TFAA), $CHCl_3$, rt, overnight, 62%; (d) Zn, 3N HCl, CH_3OH, ice bath, 1 h, 43%.

intraperitoneal injection, suggesting that the pharmacokinetic (PK) profiles of these amidoalkylindoles were not optimal and still had some room for improvement.

In our efforts to discover novel and selective CB2 receptor agonists, a series of 1*H*-pyrazole-3-carboxamide derivatives were designed to overcome the metabolic liability of *N*-alkyl indole-based synthetic cannabinoids while maintaining the major pharmacophoric elements of compound **1** (Figure 2). Pyrazole-3-carboxamide fragment is well known as a privileged skeleton in medicinal chemistry and is found in many naturally occurring or synthetic substances possessing a variety of biological functions. The methods of synthesizing 1*H*-pyrazole-3-carboxamide derivatives are flexible and reliable, which allow the rapid preparation of diverse analogues based on this moiety and facilitate the structural optimization process. Besides, it is noteworthy that the 1*H*-pyrazole-3-carboxamide scaffold has been applied in the development of CB1 receptor antagonists/inverse agonists and in PET tracers for clinical use such as **2** and [^{123}I]-AM281[44−47] (**10**), indicating that the discovery of selective CB2 receptor agonists based on 1*H*-pyrazole-3-carboxamide scaffold may be saturated with challenges and opportunities. Therefore, structural modification needs to be cautiously implemented to achieve this goal. In this work, the target compounds were initially obtained as pyrazole-3-carboxamide (1,3-regioisomer) and pyrazole-5-carboxamide (1,5-regioisomer) analogues, as exemplified by compounds **17** and **23**, to investigate which regioisomer was preferred to maintain the potency against CB2 receptor. Further structure optimization along with a series of pharmacological evaluations led to the identification of compound **66**, which is a potent and selective CB2 receptor agonist with high efficacy. In addition, compound **66** significantly attenuated dermal fibrosis in a BLM-induced mouse model of SSc, further supporting a tight interplay between the cannabinoid system and SSc.

RESULTS AND DISCUSSION

Chemistry. The syntheses of pyrazole analogues **17**−**52** and **54**−**68** were accomplished as depicted in Schemes 1 and 2. The ketones **13a**−**g** were treated with diethyl oxalate in the presence of *t*-BuOK by the Claisen condensation to afford the corresponding γ-diketo esters. These intermediates were further cyclized with hydrazine monohydrate to produce **14a**−**g**. The N-alkylation of **14a** with 1-bromopentane led to a mixture of regioisomers **15a** (29%) and **16a** (33%), which were separated by flash chromatography and characterized by heteronuclear multiple-bond coherence (HMBC) experiments (see the Supporting Information). In addition, it should be noted that the 1,3-regioisomer **16a** showed a lower R_f value compared to its 1,5-counterpart (**15a**) when monitored via thin-layer chromatography (TLC) analysis. This pattern was also applicable to all pyrazoles described in the present work. Upon ester hydrolysis, compounds **15a**−**o** and **16a**−**o** were coupled with various amines using 2-(7-aza-1*H*-benzotriazole-1-yl)-1,1,3,3-tetramethyluronium hexafluoro (HATU) to furnish the desired products **17**−**40** and **45**−**52**. Alternatively, **13a** was cyclized with different arylhydrazines to produce pyrazole-3-carboxamide intermediates **53a**−**o** as major products,[48,49] which were further transformed to final compounds **54**−**68** by employing the same strategy as described for compound **26**. In an effort to further investigate the SAR of the 4-position of pyrazole ring in compound **26**, various substituents were introduced in this position, as outlined in Scheme 2. In the presence of the radical initiator dibenzoyl peroxide, compound **26** was treated with NBS or NCS in $CHCl_3$ to afford compounds **41** and **42**, respectively. Compound **43** was obtained via nitration of compound **26**, and further reduction of the nitro group to the amino group in compound **43** provided the desired product **44**.

***In Vitro* Functional Studies.** *In vitro* functional profiles of compounds **17**−**52** and **54**−**68** against CB1 and CB2 receptors were evaluated in calcium mobilization assay through co-expressing Gα16 and human CB1 and CB2 receptors in CHO cells.[50] All of the final compounds were initially screened for their agonism activities at a concentration of 10 μM. Compounds exhibiting over 50% activation were next evaluated for their EC_{50} values. CP55940 (**11**) and AM630 (**12**) were tested concurrently as nonselective cannabinoid receptor agonist and selective CB2 receptor antagonist, respectively. Maximal efficacy (E_{max}) was determined as maximal effect relative to compound **11**. We first explored the SARs between the 1,3- and 1,5-regioisomers starting with R^1 substituents. Pyrazole-5-carboxamide analogues **17**−**20** were much less active than their counterparts **23**−**26** at both CB1 and CB2 receptors, suggesting that the 1,3-regioisomer pyrazole was preferred to maintain agonist potency at cannabinoid receptors (Table 1). Compound **23**, acting as a partial agonist, exhibited moderate activity at both CB1 and CB2 receptors ($EC_{50,CB1}$ = 270.6 nM, $EC_{50,CB2}$ = 194.2 nM). Replacing the adamantane in compound

https://dx.doi.org/10.1021/acs.jmedchem.0c01023
J. Med. Chem. 2021, 64, 385−403

Table 1. Agonist Activity of Compounds 17−34 against the Human CB1 and CB2 Receptors in Calcium Mobilization Assays[a]

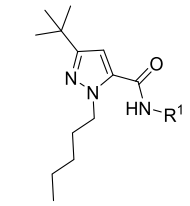

1,5-regioisomers **17 - 22**

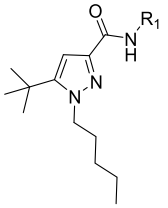

1,3-regioisomers **23 - 34**

Compd.	R^1	CB1		CB2	
		EC_{50} (nM)[b]	E_{max} (%)	EC_{50} (nM)	E_{max} (%)
17		>10^5	ND[c]	>10^5	ND
18		>10^5	ND	>10^5	ND
19		>10^5	ND	300.9 ± 50.9	80
20	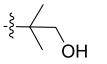	>10^5	ND	318.6 ± 5.0	80
21	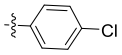	>10^5	ND	>10^5	ND
22	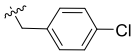	>10^5	ND	>10^5	ND
23		270.6 ± 35.9	69	194.2 ± 1.5	58
24	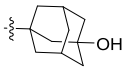	4.0 ± 0.4	100	>10^5	ND
25		7.2 ± 2.5	100	12.0 ± 5.3	100
26	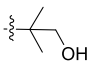	17.4 ± 1.1	100	2.9 ± 0.5	100
27	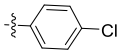	>10^5	ND	2349.5.0 ± 707.4	80
28	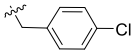	>10^5	ND	>10^5	ND
29	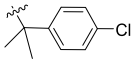	135.0 ± 11.2	100	57.0 ± 1.9	100
30		220.5 ± 4.6	30	118.4 ± 15.9	60
31		103.8 ± 19.4	50	46.0 ± 0.7	80
32	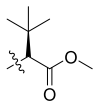	4.3 ± 0.3	100	26.1 ± 4.3	100
33	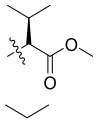	1.6 ± 0.4	90	7.4 ± 2.3	90
34	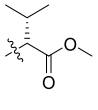	26.6 ± 0.6	70	7.2 ± 1.9	100
11	-	42.0	100	35.0	100

[a]See the Experimental Section. Data represent the mean ± standard error of the mean (SEM) values of at least three independent experiments. [b]The EC_{50} values were determined by calcium mobilization assay and calculated with GraphPad Prism 7 software. Compound **11** served as a positive control with EC_{50} values of 42.0 and 35.0 nM against the CB1 and CB2 receptors, respectively. [c]ND: not determined; for compounds with EC_{50} > 10^5 nM, their maximal effects were not determined.

https://dx.doi.org/10.1021/acs.jmedchem.0c01023
J. Med. Chem. 2021, 64, 385−403

Table 2. Agonist Activity of Compounds 35−44 against the Human CB1 and CB2 Receptors in Calcium Mobilization Assays[a,d]

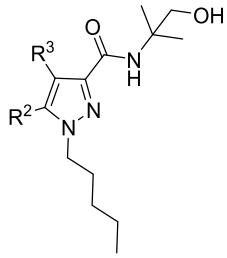

Compounds **35 - 44**

Compd.	R^2	R^3	CB1		CB2	
			EC_{50} (nM)	E_{max} (%)[b]	EC_{50} (nM)	E_{max} (%)
35		H	187.5 ± 57.8	80	53.8 ± 13.2	80
36		H	170.6 ± 44.9	90	38.5 ± 8.6	70
37		H	27. 0 ± 8.1	90	12.0 ± 1.1	50
38		H	>10^5	ND[c]	>10^5	ND
39		H	>10^5	ND	>10^5	ND
40[d]	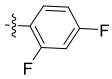	H	>10^5	ND	>10^5	ND
41		Cl	33.9 ± 21.6	50	3.4 ± 0.7	100
42		Br	27.0 ± 3.1	50	2.0 ± 0.8	100
43		NO_2	128.6 ± 6.8	100	13.3 ± 0.8	70
44		NH_2	195.3 ± 44.2	80	5.5 ± 25.1	100
11	-	-	42.0	100	35.0	100

[a]See the Experimental Section. Data represent the mean± SEM values of at least three independent experiments. [b]The EC_{50} values were determined by calcium mobilization assay and calculated with GraphPad Prism 7 software. Compound **11** served as a positive control with EC_{50} values of 42.0 and 35.0 nM against the CB1 and CB2 receptors, respectively. [c]ND: not determined; for compounds with EC_{50} > 10^5 nM, maximal effects were not further determined. [d]All of the final compounds were tested for their antagonist activity at the CB2 receptor, and only compound **40** behaved as a selective antagonist at the CB2 receptor (IC_{50} = 87.1 nM). Cells were preincubated with tested compounds at different concentrations for 15 min, followed by the addition of compound **11** (100 nM).

23 with an aromatic group such as 4-chlorophenyl (**27**) or 4-chlorobenzyl (**28**) resulted in a further loss of activity, with the exception of pyridine analogue **30** which exhibited a slightly better functional activity than compound **23** at both receptors. However, compound **29** with two methyl groups in the *α*-position of the 4-Cl-phenyl was about 2- to 3-fold more potent compared to compound **23** at both CB1 and CB2 receptors. Unexpectedly, introduction of a hydroxyl group into the adamantane of compound **23** resulted in a selective CB_1 receptor agonist **24** (EC_{50} = 4.0 nM). In consideration of monohydroxylation of the adamantyl moiety being one of the primary metabolic pathways for **1** and its analogues,[43] it is likely that these monohydroxylated metabolites also behave as potent CB1 receptor agonists. On the other hand, the alkyl-substituted compounds **25**, **26**, and **31** displayed a significant increase of potency in comparison to compound **23** at both receptors. In particular, the terminal alcohol **26** acted as a high efficacy agonist with low nanomolar activities at both receptors and showed a fivefold preference for CB2 receptor ($EC_{50,CB1}$ = 17.4 nM, $EC_{50,CB2}$ = 2.9 nM). In addition, although introducing D/L amino acid methyl esters such as leucine or valine (**32**−**34**) was beneficial for functional potency at both receptors, compound **33** was readily degraded in human liver microsomal stability assay (Table 4).

As compound **26** was the most promising hit obtained so far, our subsequent SAR studies focused on the R^2 and R^3 positions in the pyrazole ring (Table 2). Replacing the *tert*-butyl in compound **26** with a trifluoromethyl (**35**), isopropyl (**36**), or neopentyl (**37**) group resulted in varying decreases of potency at CB2, while the efficacy and selectivity of these analogues declined as well. In addition, the cycloalkyl substitutions (**38** and **39**) yield a total loss of agonistic activity against both receptors. Interestingly, a 2,4-difluorophenyl substitution resulted in a selective CB2 receptor antagonist **40** (IC_{50} = 87.1 nM). Next, pyrazole ring 4-position substituents were investigated. As shown in Table 2, introduction of various substituents

https://dx.doi.org/10.1021/acs.jmedchem.0c01023
J. Med. Chem. 2021, 64, 385−403

Table 3. Agonist Activity of Compounds 45−52 and 54−68 against the Human CB1 and CB2 Receptors in Calcium Mobilization Assays[a]

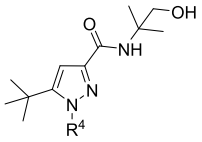

Compounds **45 - 52** and **54 - 68**

Compd.	R^4	CB1		CB2	
		EC_{50} (nM)[b]	E_{max} (%)	EC_{50} (nM)	E_{max} (%)
45		>10^5	ND[c]	209.8±32.7	100
46		100.8 ± 13.0	90	10.1 ± 1.1	100
47		47.0 ± 13.4	100	13.4 ± 1.9	100
48		>10^5	ND	184.1 ± 25.5	100
49		285.3 ± 36.8	100	65.9 ± 7.9	100
50	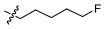	43.0 ± 11.4	90	36.4 ± 5.4	70
51		4899.7 ± 262.7	20	103.2 ± 0.3	100
52		>10^5	ND	>10^5	ND
54		>10^5	ND	>10^5	ND
55		>10^5	ND	197.3 ± 58.6	40
56		>10^5	ND	685.1 ± 16.5	82
57		>10^5	ND	203.7 ± 21.6	100
58		>10^5	ND	>10^5	ND
59	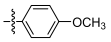	>10^5	ND	>10^5	ND
60	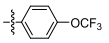	>10^5	ND	>10^5	ND
61	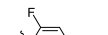	>10^5	ND	1725.0 ± 242.8	80
62		>10^5	ND	3890.7 ± 1646.4	80
63		>10^5	ND	>10^5	ND
64		>10^5	ND	135.4 ± 7.0	100
65		>10^5	ND	731.3 ± 192.9	50
66		1839.0 ± 541.3	30	15.2 ± 2.1	100
67	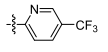	>10^5	ND	>10^5	ND
68		>10^5	ND	>10^5	ND
11	-	42.0	100	35.0	100

[a]See the Experimental Section. Data represent the mean ± SEM values of at least three independent experiments. The EC_{50} values were determined by calcium mobilization assay and calculated with GraphPad Prism 7 software. Compound **11** served as a positive control with EC_{50} values of 42.0 and 35.0 nM against the CB1 and CB2 receptors, respectively. [b]ND: not determined; for compounds with EC_{50} > 10^5 nM, their maximal effects were not determined.

(compounds **41**−**44**) in this position was well tolerated and the agonist activity of these derivatives at the CB2 receptor remained at a low nanomolar level. With the exception of nitro analogues **43**, these compounds behaved as high-efficacy agonists toward the CB2 receptor and exhibited improved selectivity over the CB1 receptor compared to parent compound **26**.

Finally, in an attempt to further improve CB2 receptor selectivity and PK properties, the R^4 substituent of compound **26** was interrogated. As shown in Table 3, shortening or extending the pentyl side chain in the N-1 position of compound **26** with one carbon atom (**46** and **47**) was tolerated for CB2 agonist activity, while the two carbon shorter homologue **45** showed a distinct reduction in CB2 receptor agonist activity and was completely inactive at the CB1 receptor. In comparison to their parent compounds, terminal fluorinated analogues (**48**, **49**, and **50**) were generally less active and selective at the CB2 receptor. Replacement of the pentyl substituent in compound **26** with a cyclopropylmethyl (**51**) or 2-methoxyethyl (**52**) group led to a significant drop of agonistic activity at both receptors.

Since *N*-dealkylation was one of the main metabolic pathways for compound **1** and its derivatives,[43] a series of aryl substituents were introduced into the *N*-1 position of compound **26** for improving the metabolic stability of these pyrazole-3-carboxamide ligands. Unfortunately, compound **54**, possessing a phenyl ring in the *N*-1 position, was found to be totally inactive toward both CB1 and CB2 receptors. However, further structural optimization demonstrated that various substituents attached to the benzene ring of compound **54** had a considerable effect on its agonist potency against the CB2 receptor. For instance, the 2,4-difluoro substitution yielded a selective CB2 receptor agonist **61** with an EC_{50} value of 1725 nM, and mono-substitutions at the para-position resulted in compounds **55**−**57** that were 2- to 8-fold more active than compound **61**, while compounds **58**−**60** completely lost their cannabinoid receptor activities. In the field of medicinal chemistry, the substitution of a CH group with a nitrogen atom in an aromatic system is a common strategy to improve the biochemical potency and physicochemical profiles of targeted molecules.[51] In this study, incorporation of a nitrogen atom at the 2-position of the phenyl ring (**62**) was beneficial for CB2 receptor activity compared to parent compound **55**, while its 3-pyridine analogue **63** and pyrimidine analogue **68** were inactive against both cannabinoid receptors. Introduction of substituents at the 4-position of phenyl in compound **62** greatly improved the agonist activity toward the CB2 receptor (compounds **64**−**66**); in particular, the trifluoromethyl analogue **66** exhibited low nanomolar CB2 agonist potency and more than 100-fold selectivity over CB1 receptor ($EC_{50,CB1}$ = 1839 nM, $EC_{50,CB2}$ = 15.2 nM). Meanwhile, it behaved as a high-efficacy CB2 receptor agonist and a weak agonist at the CB1 receptor (E_{max} = 30%), and its CB2 agonist

https://dx.doi.org/10.1021/acs.jmedchem.0c01023
J. Med. Chem. 2021, 64, 385−403

activity could be effectively blocked by a selective CB2 antagonist AM630 (Figure S1). Further modification afforded compound **67** with an extra chlorine atom at the 6-position of pyridine ring, which was entirely ineffective at both receptors.

To further explore the interactions between **66** and **40** with CB2 receptor and characterize the different binding modes, we conducted molecular docking studies for **66** on active CB2 (PDB code: 6PT0)[52] and **40** on inactive CB2 (PDB code: 5ZTY).[53] The docking poses of **66** and **40** are quite similar in the orthostatic binding pocket along with the key interacting residues (Figure 3). The −OH moiety of both compounds can

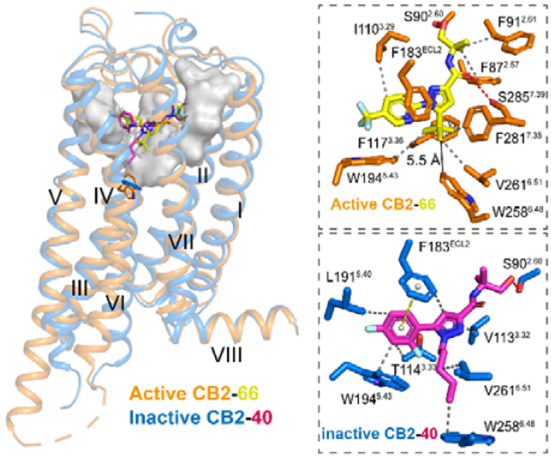

Figure 3. Comparison of docking results of agonist **66** on active CB2 receptor (PDB code: 6PT0) and antagonist **40** on inactive CB2 receptor (PDB code: 5ZTY). (Left) Superposition of docking poses of agonist **66** (yellow) on activated CB2 (orange) and antagonist **40** (magenta) on inactive CB2 receptor (sky blue). (Right) Detailed interactions of the **66** (top) or **40** (bottom) on CB2 receptor.

form a hydrogen bond with residue S90$^{2.60}$, the pyridine moiety from compound **66** and benzene moiety from compound **40** are predicted to form strong $\pi-\pi$ interactions with F183^{ECL2} and hydrophobic interactions with W194$^{5.43}$ and V261$^{6.51}$. Moreover, F87$^{2.57}$, F91$^{2.61}$, I110$^{3.29}$, F117$^{3.36}$, F281$^{7.35}$, and S285$^{7.39}$ are important for recognition of the CB2 agonist **66**, and F83^{ECL2}, V113$^{3.32}$, T114$^{3.33}$, and L191$^{5.40}$ via hydrophobic interactions with compound **40**. The most different feature is that the agonist **66** does not extend sufficiently deep to constrain the conformation of W258$^{6.48}$ with a distance of 5.5 Å, whereas the alkyl chain of compound **40** approaches closer to W258$^{6.48}$ to form potentially hydrophobic interactions (Figure 3).

***In Vitro* Metabolic Stability and *In Vivo* PK Study.** To assess the metabolic stability of synthesized 1*H*-pyrazole-3-carboxamide derivatives, selected compounds were initially tested in the human liver microsome assay *in vitro*. As shown in Table 4, compound **66** exhibited a much better metabolic stability profile than other four compounds, with a half-time of nearly 2 h and at least 64% of the parent compound remained upon 1 h incubation at a concentration of 10 μM. Apparently, introduction of a pyridyl in the *N*-1 position of pyrazole notably improved metabolic stability. However, compounds bearing an amino acid methyl ester group or an amino group in the 4-position of the pyrazole were less stable than the parent compound (**33** vs **26**, **44** vs **26**).

Next, the preliminary *in vivo* PK profiles of **66** were further characterized *in vivo*. Compound **66** was intravenously or orally administered at 1 or 5 mg/kg (Balb/c mice). As depicted in

Table 4. Human Liver Microsome Stability Data for Compounds 26, 33, 40, 44, and 66

compd.	$t_{1/2}$[a] (min)	$CL_{int(mic)}$[b] (μL/min/mg)	$CL_{int(liver)}$[c] (mL/min/kg)	remaining (T = 60 min)
26	22.2	62.4	56.1	14.9%
33	11.8	117.0	105.3	2.9%
40	21.4	64.6	58.2	14.1%
44	13.3	104.4	94.0	4.6%
66	112.6	12.3	11.1	64.0%
testosterone	18.8	73.6	66.3	10.7%
diclofenac	10.8	128.9	116.0	2.0%
propafenone	7.3	189.1	170.2	0.4%

[a] $t_{1/2}$, half-life. [b] $CL_{int(mic)}$, intrinsic clearance, 0.693/half-life/mg microsome protein per mL. [c] $CL_{int(liver)}$ = $CL_{int(mic)}$ × microsomal protein/liver weight (mg/g) × liver weight/body weight (g/kg).

Table 5, compound **66** demonstrated an acceptable half-life ($t_{1/2}$ = 130.8 min) and favorable drug exposure ($AUC_{0-\infty}$ = 1672.9 ng·h/mL), as well as excellent oral bioavailability (F = 79.5%) when dosed orally. In general, compound **66** exhibited a favorable PK profile and was suitable for further animal efficacy studies.

***In Vitro* Pharmacological Characterization of Compound 66.** Previous studies have reported that CB2 receptor activation typically suppresses the formation of intracellular cyclic adenosine monophosphate (cAMP) via inhibiting adenylyl cyclase activity.[54] Compound **66** was chosen to be evaluated in an HTRF-based cAMP assay using CHO cells expressing CB2 (Figure 4A,B). Compound **66** significantly inhibited cAMP production (EC_{50} = 10.7 nM), which was more potent than that of positive control **11** (EC_{50} = 16.3 nM) and in line with the results obtained from the calcium mobilization assay (**66**, $EC_{50,CB2}$ = 15.2 nM; **11**, $EC_{50,CB2}$ = 35.0 nM). Extracellular signal-regulated kinase (ERK) is a key cellular effector of GPCR activation.[54] We then detected ERK activation in CHO cells transiently transfected with CB2 expression or empty vector. As shown in Figure 4C,D, compound **66** induced ERK phosphorylation in CHO cells co-expressing CB2, but not in negative control with empty vector. The effects of compound **66** were completely inhibited by a specific CB2 receptor antagonist AM630. Activation of cannabinoid receptors is capable of stimulating G-protein-independent β-arrestin signaling pathway. To evaluate whether **66** was able to affect the CB1- or CB2-dependent β-arrestin2 trafficking, a typical Tango β-arrestin recruitment assay was used to assess GPCR activation.[55] As shown in Figure S2, positive control **11** exhibited high potency against both CB1 and CB2 receptors($EC_{50,CB1}$ = 0.3 nM, $EC_{50,CB2}$ = 9.8 nM). Compound **66** was not active in CB1-TANGO assay (EC_{50} > 10 μM). On the contrary, it dose-dependently induced β-arrestin2 trafficking in HEK293-CB2 cells (EC_{50} = 561.6 nM), suggesting that compound **66** was biased toward G-protein signaling at the CB2 receptor (calcium mobilization assay: EC_{50} = 15.2 nM). Moreover, compound **66** was evaluated in a series of endocannabinoid-related GPCRs (GPR119, GPR132, and prostaglandin EP2 and EP4 receptors), and it exhibited neither agonist nor antagonist activity against these receptors at 10 μM (data not shown). Taken together, these findings suggested that compound **66** activated a range of downstream signaling pathways specifically through CB2 receptors.

Moreover, it has been reported previously that repeated stimulation of a GPCR with its agonist leads to receptor

https://dx.doi.org/10.1021/acs.jmedchem.0c01023
J. Med. Chem. 2021, 64, 385−403

Table 5. Preliminary PK Parameters of Compound 66 *In Vivo*

route	dose (mg/kg)	C_{max} (ng/mL)	$AUC_{0-\infty}$ (ng·h/mL)	Vd (L/kg)	CL (L/h/kg)	$t_{1/2}$ (min)	*F* (%)
iv	1	959.1	422.0	4.5	2.4	79.2	
po	5	603.0	1672.9	9.2	3.1	130.8	79.5

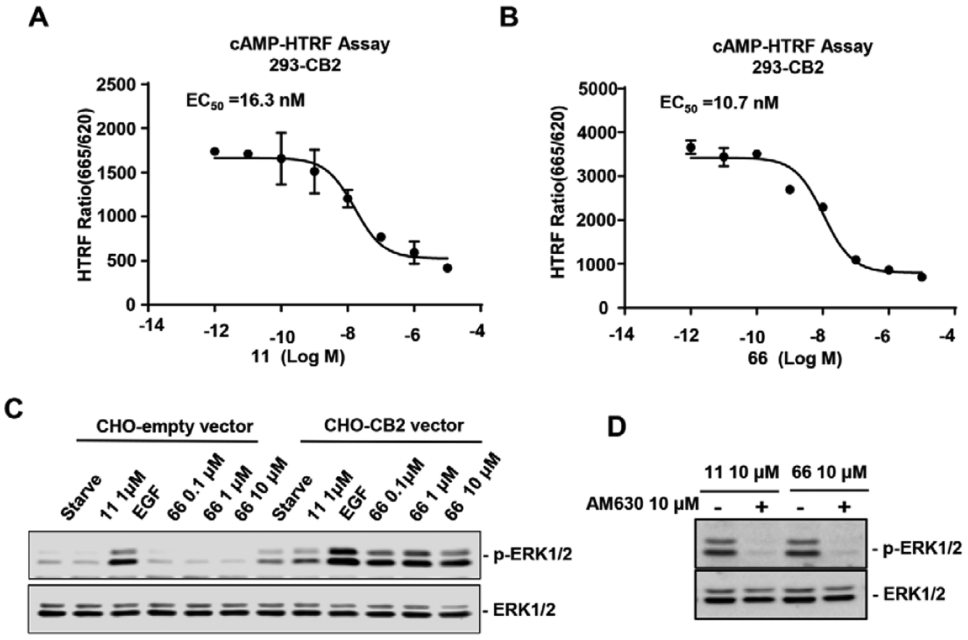

Figure 4. *In vitro* functional activity of compound **66**. (A, B) Compounds **11** and **66** inhibited cAMP formation that is stimulated by forskolin in the CB2-expressing CHO cells as determined by HTRF assay. Data represent the mean ± SEM values of at least three independent experiments. (C, D) Cells were subjected to indicated treatments, and extracellular signal-regulated kinase1/2 (ERK1/2) phosphorylation was detected by Western blotting. EGF: epidermal growth factor.

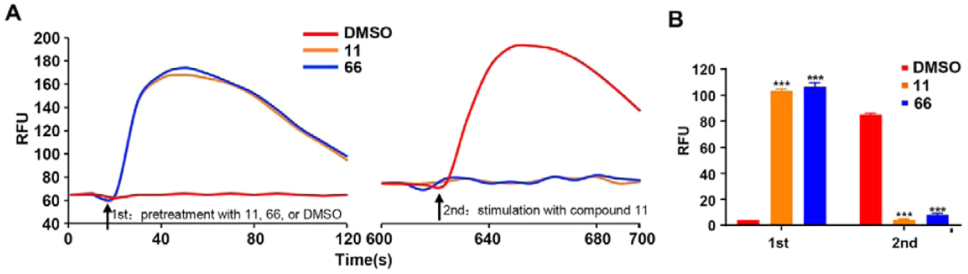

Figure 5. Compound **66** induced desensitization of CB2 receptor. CHO-CB2-Gα16 cells were initially stimulated with 10 μM compound **11**, compound **66**, or DMSO (0.1%), and the intracellular calcium response was detected (left). The cells were washed with HBSS buffer upon incubation for 10 min and restimulated (right, second arrow) with compound **11** (10 μM). Representative intracellular calcium signals were present with at least three independent measurements. (B) Quantitative analysis, the significance of the difference was assessed via unpaired two-tailed Student's *t*-test. ***, $p < 0.001$.

desensitization, which is a protective mechanism to restrict constant GPCR activation.[30,56] To determine whether compound **66** was capable of inducing CB2 desensitization, CHO-CB2-Gα16 cells were first stimulated with tested compounds (10 μM) or dimethyl sulfoxide (DMSO, 0.1%). As shown in Figure 5, compounds **11** and **66** both caused a significant increase in intracellular calcium concentration. The cells were washed with HBSS buffer upon 10 min incubation and then restimulated with 10 μM compound **11**. The cells pretreated with 0.1% DMSO responded sufficiently to the stimulation of compound **11**, while the cells pretreated with compounds **11** or **66** displayed a distinct decline in calcium response following the second stimulus.

Antifibrotic Effects of Compound 66 in a Mouse Model of SSc. Encouraged by the favorable pharmacological properties *in vitro* and PK profile *in vivo*, compound **66** was next selected for further *in vivo* characterization in a BLM-induced mouse model of SSc. Upon subcutaneous injections of BLM for 2 weeks, dermal fibrosis was induced in the back skin of the Balb/c mice. Compound **9** was used as a positive control for the animal study due to its well-documented *in vivo* antifibrotic activity.[50] The mice were subsequently treated with compound **66** (1 or 5 mg/kg/day) or **9** (1 mg/kg/day) for another 4 weeks. Skin fibrosis was characterized by determining the dermal thickness and collagen deposition. As shown in Figure 6A,B, BLM treatment resulted in a remarkable increase in dermal thickness and dermal collagen deposition (sirius red positive area) compared to the

https://dx.doi.org/10.1021/acs.jmedchem.0c01023
J. Med. Chem. 2021, 64, 385−403

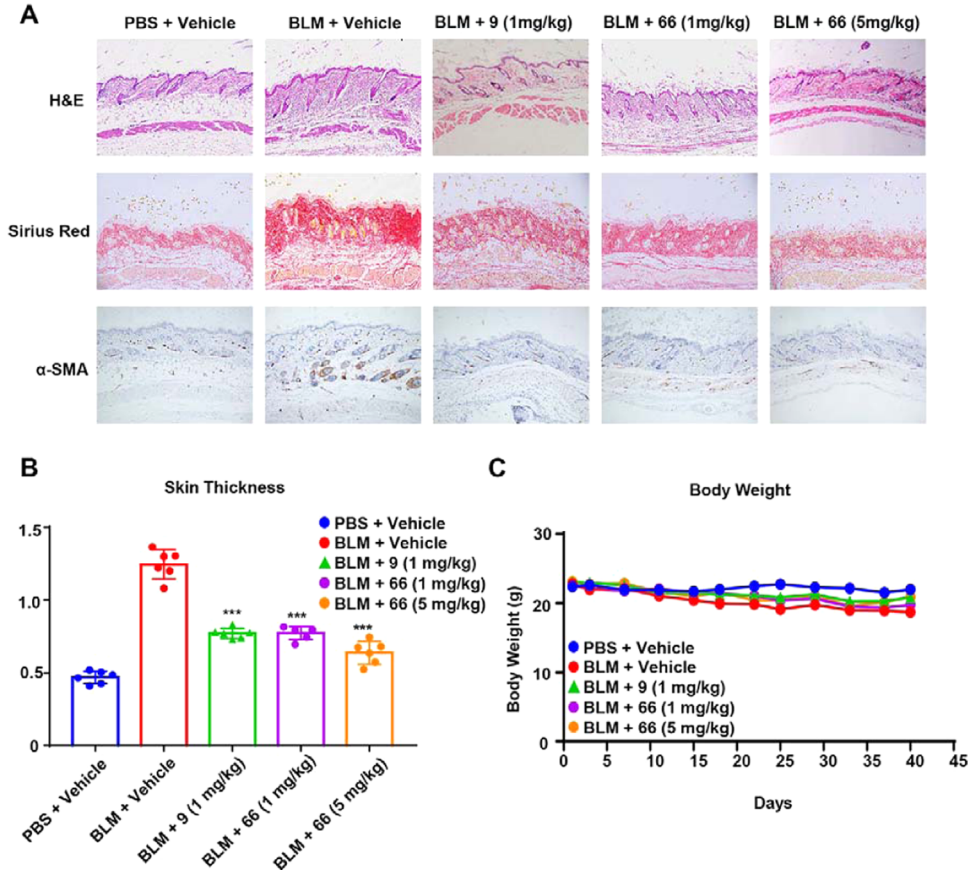

Figure 6. Compound **66** alleviated BLM-induced dermal fibrosis and inflammation in mice. (A) H&E, sirius red, and α-SMA immunohistochemistry staining of skin sections with scale bar of 200 μm. (B) Dermal thickness data were measured at the end of the experiment (shown as mean ± standard deviation (SD), $n = 8$). (C) Body weight was measured twice a week. The significance of the difference between mean values was evaluated using one-way analysis of variance (ANOVA) followed by Tukey's multiple comparison test. ***, $P < 0.001$.

control group. In compound **66**-treated groups, BLM-induced dermal pathological symptoms were significantly attenuated and the skin thickness in the high-dose group was reduced nearly to the control level. Meanwhile, immunohistochemical analysis results demonstrated that compound **66** could also dramatically decrease the expression of α-smooth muscle actin (α-SMA), one of the key cellular mediators of fibrosis in SSc. In addition, no significant body weight loss was observed in mouse cohorts, suggesting that compound **66** was well tolerated at the tested dosages (Figure 6C). Moreover, it was found that BLM significantly increased the mRNA expression of a series of proinflammatory and fibrotic mediators such as Col1α, α-SMA, TNF-α, and TGF-β in skin lesions, which was markedly suppressed after **66** treatment (Figure 7) in a dose-dependent manner. Collectively, these data demonstrated that compound **66** could effectively attenuate both dermal inflammation and fibrosis in a BLM-induced mouse model of SSc.

CONCLUSIONS

In summary, we prepared a series of novel 1*H*-pyrazole-3-carboxamide derivatives to develop selective CB2 agonists that lacked CB1 associated psychiatric side effects. Initial screening of compounds **17**−**34** revealed that the 1,3-regioisomer pyrazoles were preferred to maintain agonist activity at cannabinoid receptors. Further structural modifications to improve the potency, selectivity, and PK profiles of designed compounds resulted in identifying the most promising compound **66** as a highly potent and selective CB2 receptor agonist. In addition, compound **66** exhibited good metabolic stability and favorable PK properties both *in vitro* and *in vivo* that warranted its subsequent animal efficacy study. In a BLM-induced mouse model of SSc, subcutaneous injections of compound **66** at 1 or 5 mg/kg for 4 weeks significantly relieved BLM-induced dermal thickness and collagen deposition, as well as suppressed the mRNA expression of a series of pro-inflammatory and fibrotic mediators such as Col1α, α-SMA, TNF-α, and TGF-β in skin lesions. Together, this evidence suggested that compound **66** effectively delayed fibrosis progress and is expected to be a potential preclinical candidate for the treatment of SSc.

EXPERIMENTAL SECTION

Chemistry. *General.* All anhydrous solvents, starting materials, and reagents were purchased from commercial sources and used without any further purification. Reactions in this work were run under a N_2 atmosphere. All reactions were monitored using TLC on SiO_2 and visualized with UV light. NMR spectra were recorded on Bruker 400, 500, or 600 MHz instruments. The values of chemical shifts were shown in δ (ppm) using DMSO-d_6 (2.50 and 39.51 ppm) or $CDCl_3$ (7.26 and 77.00 ppm) as the standard. Mass spectra (MS) were obtained on GCMS-QP2010 in electrospray ionization (ESI) mode, while high-resolution mass spectra (HRMS) were obtained using a Bruker Micro TOF-Q II liquid chromatography-mass spectrometry (LC-MS) instrument in ESI mode. Melting points (mp) were determined on an SGWX-4/4A/4B capillary apparatus. Compound purities were detected using high-pressure liquid chromatography (Agilent Technologies 1200 Series) with an ACE Excel 5 C18 column (5 μm, 4.6 mm

https://dx.doi.org/10.1021/acs.jmedchem.0c01023
J. Med. Chem. 2021, 64, 385−403

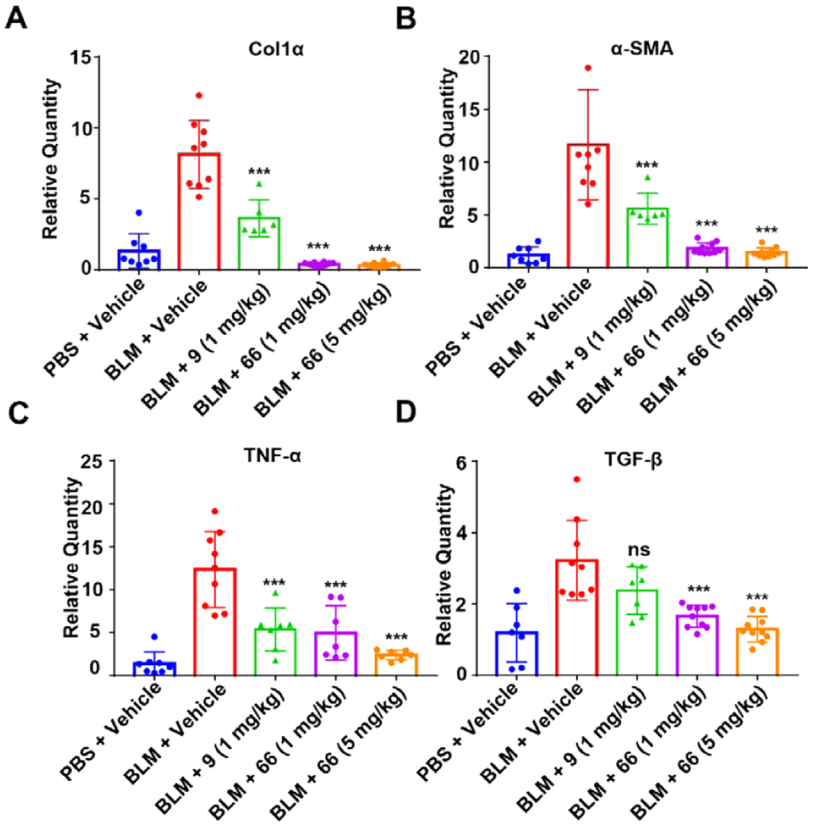

Figure 7. mRNA expression levels of Col1α (A), α-SMA (B), TNF-α (C), and TGF-β (D) in skin lesions. Data are shown as mean ± SD, $n = 8$. The significance between different groups was assessed using one-way ANOVA followed by Bonferroni's multiple comparison test. *, $P < 0.05$, **, $P < 0.01$, ***, $P < 0.001$.

× 250 mm) at 40 °C with a flowrate of 1.5 mL/min. The detection was done at 254 or 280 nm on a G1314B detector. Gradient A, 20−90% CH_3OH in water over 20 min; gradient B, 20−40% CH_3OH (0−5 min), 40−90% CH_3OH (5−7 min), 90% CH_3OH (7−15 min), 90−20% CH_3OH (15−20 min). All of the final biologically tested compounds had a confirmed purity of ≤95%.

General Synthetic Procedure of *N*-alkyl-Substituted Pyrazoles. *Ethyl 5-(tert-Butyl)-1H-pyrazole-3-carboxylate (**14a**).* To a solution of 3,3-dimethyl-2-butanone (1.0 g, 10.0 mmol) in anhydrous THF (250 mL) was added *t*-BuOK (1.46 mg, 13.0 mmol) with ice cooling. After stirring for 10 min, diethyl oxalate (1.36 mL, 10.0 mmol) was added and the reaction mixture was refluxed for 5 h. Then, hydrazine hydrate (550 mg, 11.0 mmol) was added dropwise to the mixture, followed by the addition of AcOH (1.5 mL). The mixture was stirred at 60 °C for 3 h. Then, the reaction was concentrated under vacuum and the crude mixture was extracted with EtOAc. The combined organic layers were washed with brine, dried over anhydrous Na_2SO_4, and concentrated. The resulted residue was purified by flash chromatography on silica gel to give the title compound **14a** (1.54 g, 78.3%). ^{1}H NMR (500 MHz, DMSO-d_6) δ 13.21 (s, 1H), 6.46 (s, 1H), 4.31−4.19 (m, 2H), 1.28 (m, 12H).

*Ethyl 3-(tert-Butyl)-1-pentyl-1H-pyrazole-5-carboxylate (**15a**) and Ethyl 5-(tert-Butyl)-1-pentyl-1H-pyrazole-3-carboxylate (**16a**).* To a solution of **14a** (564 mg, 2.88 mmol) in anhydrous THF (30 mL) was added *t*-BuOK (337 mg, 3.45 mmol) with ice cooling. Then, 1-bromopentane (0.43 mL, 3.45 mmol) was slowly added and the mixture was refluxed overnight. The reaction was cooled to room temperature (rt) and concentrated under vacuum. The crude mixture was extracted with EtOAc, and the combined organic layers were washed with brine, dried over anhydrous Na_2SO_4, and concentrated. The residue was purified by flash chromatography on silica gel to give the isomer compound ethyl 3-(*tert*-butyl)-1-pentyl-1*H*-pyrazole-5-carboxylate (406 mg, 29%) and compound ethyl 5-(*tert*-butyl)-1-pentyl-1*H*-pyrazole-3-carboxylate (220 mg, 33%). Ethyl 3-(*tert*-butyl)-1-pentyl-1*H*-pyrazole-5-carboxylate (**15a**): ^{1}H NMR (500 MHz, $CDCl_3$) δ 6.55 (s, 1H), 4.45−4.33 (m, 2H), 4.25−4.15 (m, 2H), 1.96 (m, 2H), 1.43−1.32 (m, 16H), 0.93 (t, $J = 6.1$ Hz, 3H). Ethyl 5-(*tert*-butyl)-1-pentyl-1*H*-pyrazole-3-carboxylate (**16a**): ^{1}H NMR (500 MHz, $CDCl_3$) δ 6.69 (s, 1H), 4.50 (t, $J = 7.4$ Hz, 2H), 4.34 (q, $J = 7.1$ Hz, 2H), 1.82 (m, 2H), 1.40 (t, $J = 7.1$ Hz, 3H), 1.37−1.28 (m, 13H), 0.90 (t, $J = 6.6$ Hz, 3H).

*N-(1-Adamantyl)-3-(tert-butyl)-1-pentyl-1H-pyrazole-5-carboxamide (**17**).* A solution of **15** (78 mg, 0.29 mmol) and LiOH·H_2O (74 mg, 1.76 mmol) in 10 mL of MeOH:H_2O:THF = 2:1:2 was stirred at rt for 1 h. The reaction was then concentrated under vacuum and acidified to pH 4−5 with 1 M aqueous HCl. The mixture was extracted with EtOAc, and the combined organic layers were washed with brine, dried over anhydrous Na_2SO_4, and concentrated to afford the crude compound 3-(*tert*-butyl)-1-pentyl-1*H*-pyrazole-5-carboxylic acid. To a solution of 3-(*tert*-butyl)-1-pentyl-1*H*-pyrazole-5- carboxylic acid (72 mg, 0.30 mmol) and 1-adamantylamine in CH_2Cl_2 (5 mL) was added HATU (137 mg, 0.36 mmol), followed by DIPEA (0.1 mL, 0.60 mmol). The mixture was stirred at rt for 5 h. Then, the reaction was concentrated under vacuum and the crude mixture was extracted with EtOAc. The combined organic layers were washed with brine, dried over anhydrous Na_2SO_4, and concentrated. The residue was purified by flash chromatography on silica gel to give the title compound **17** (62 mg, 68.8%) as a white solid. ^{1}H NMR (500 MHz, $CDCl_3$) δ 6.19 (s, 1H), 5.62 (s, 1H), 4.43 (t, $J = 7.4$ Hz, 2H), 2.12−2.09 (m, 9H), 1.80−1.76 (m, 2H), 1.75−1.68 (m, 6H), 1.29−1.25 (m, 13H), 0.87 (t, $J = 6.9$ Hz, 3H). ^{13}C NMR (101 MHz, $CDCl_3$) δ 161.5, 152.8, 145.6, 103.6, 51.6, 51.5, 41.7 (3C), 36.5 (3C), 31.4, 30.5, 30.1 (3C), 29.5, 29.0 (3C), 22.4, 14.0. HRMS (ESI): calcd for $C_{23}H_{37}N_3NaO$ $[M + Na]^+$, 394.2834; found 394.2801. mp: 136−138 °C. HPLC purity = 97.9%; t_R = 11.6 min.

*3-(tert-Butyl)-N-(3-hydroxyadamantan-1-yl)-1-pentyl-1H-pyrazole-5-carboxamide (**18**).* The title compound was prepared by the same procedure described for **17** except using 3-amino-1-adamantanol instead of 1-adamantylamine as a white solid. ^{1}H NMR (500 MHz,

https://dx.doi.org/10.1021/acs.jmedchem.0c01023
J. Med. Chem. 2021, 64, 385−403

$CDCl_3$) δ 6.20 (s, 1H), 5.69 (s, 1H), 4.44−4.41 (m, 2H), 2.32 (s, 2H), 2.01 (s, 2H), 2.00 (s, 4H), 1.74−1.72 (m, 4H), 1.64−1.54 (m, 4H), 1.29−1.24 (m, 13H), 0.89 (t, J = 7.1 Hz, 3H). ^{13}C NMR (126 MHz, DMSO-d_6) δ 159.9, 158.8, 136.5, 103.9, 67.8, 54.6, 50.5, 49.3, 44.7, 35.3, 32.1, 30.9 (3C), 30.5 (2C), 30.4, 28.6 (2C), 22.1 (2C), 14.4 (2C). HRMS (ESI): calcd for $C_{23}H_{37}N_3NaO_2$ [M + Na]$^+$, 410.2783; found 410.2758. mp: 143−145 °C. HPLC purity = 99.9%; t_R = 11.5 min.

*N,3-Di-tert-butyl-1-pentyl-1H -pyrazole-5-carboxamide (**19**).* The title compound was prepared by the same procedure described for **17** except using *tert*-butylamine instead of 1-adamantylamine as a white solid. ^{1}H NMR (500 MHz, $CDCl_3$) δ 6.19 (s, 1H), 5.75 (s, 1H), 4.45−4.42 (m, 2H), 1.82−1.76 (m, 2H), 1.44 (s, 9H), 1.31−1.25 (m, 13H), 0.87 (t, J = 7.1 Hz, 3H). ^{13}C NMR (126 MHz, DMSO-d_6) δ 160.2, 158.8, 136.6, 103.8, 51.4, 50.4, 32.1, 30.9 (3C), 30.4, 29.0 (3C), 28.6, 22.1, 14.3. HRMS (ESI): calcd for $C_{17}H_{32}N_3O$ [M + H]$^+$, 294.2545; found 294.2546. mp: 118−120 °C. HPLC purity = 95.1%; t_R = 8.9 min.

*3-(tert-Butyl)-N-(1-hydroxy-2-methylpropan-2-yl)-1-pentyl-1H-pyrazole-5-carboxamide (**20**).* The title compound was prepared by the same procedure described for **17** except using 2-amino-2-methyl-1-propanol instead of 1-adamantylamine as a white solid. ^{1}H NMR (500 MHz, $CDCl_3$) δ 6.24 (s, 1H), 6.00 (s, 1H), 4.44−4.41 (m, 2H), 3.67 (s, 2H), 1.81−1.75 (m, 2H), 1.39 (s, 6H), 1.33−1.23 (m, 13H), 0.88 (t, J = 7.2 Hz, 3H). ^{13}C NMR (151 MHz, $CDCl_3$) δ 161.0, 159.9, 135.3, 102.6, 70.5, 56.5, 51.2, 32.0, 30.5, 30.5 (3C), 28.7, 24.5 (2C), 22.3, 14.0. HRMS (ESI): calcd for $C_{17}H_{32}N_3O_2$ [M + H]$^+$, 310.2495; found 310.2496. mp: 136−138 °C. HPLC purity = 96.1%; t_R = 8.6 min.

*3-(tert-Butyl)-1-pentyl-N-(4-chlorophenyl)-1H-pyrazole-5-carboxamide (**21**).* The title compound was prepared by the same procedure described for **17** except using 4-chloroaniline instead of 1-adamantylamine as a white solid. ^{1}H NMR (600 MHz, $CDCl_3$) δ 8.71 (s, 1H), 7.66 (d, J = 8.8 Hz, 2H), 7.31 (d, J = 8.8 Hz, 2H), 6.63 (s, 1H), 4.25−4.13 (m, 2H), 2.02−1.93 (m, 2H), 1.47−1.37 (m, 13H), 0.96 (t, J = 6.9 Hz, 3H). ^{13}C NMR (151 MHz, $CDCl_3$) δ 160.2, 153.5, 144.4, 136.7, 128.9 (2C), 128.62, 120.8 (2C), 104.2, 51.7, 31.5, 30.4, 30.1 (3C), 29.0, 22.4, 14.0. HRMS (ESI): calcd for $C_{19}H_{27}ClN_3O$ [M + H]$^+$, 348.1843; found 348.1836. mp: 136−138 °C. HPLC purity = 96.3%; t_R = 9.7 min.

*3-(tert-Butyl)-1-pentyl-N-(4-chlorobenzyl)-1H-pyrazole-5-carboxamide (**22**).* The title compound was prepared by the same procedure described for **17** except using 4-chlorobenzylamine instead of 1-adamantylamine as a white solid. ^{1}H NMR (500 MHz, DMSO-d_6) δ 8.96−8.90 (m, 1H), 7.38 (d, J = 8.5 Hz, 2H), 7.32 (d, J = 8.5 Hz, 2H), 6.73 (s, 1H), 4.45−4.34 (m, 4H), 1.72−1.59 (m, 2H), 1.27−1.21 (m, 11H), 1.18−1.12 (m, 2H), 0.81 (t, J = 7.2 Hz, 3H). ^{13}C NMR (126 MHz, DMSO-d_6) δ 160.0, 159.2, 138.9, 135.2, 131.8, 129.6 (2C), 128.7 (2C), 103.8, 50.7, 41.9, 32.1, 30.9 (3C), 30.5, 28.6, 22.1, 14.3. HRMS (ESI): calcd for $C_{20}H_{29}ClN_3O$ [M + H]$^+$, 362.1999; found 362.2001. mp: 136−138 °C. HPLC purity = 98.6%; t_R = 9.2 min.

*N-(1-Adamantyl)-5-(tert-butyl)-1-pentyl-1H-pyrazole-3-carboxamide (**23**).* A solution of **16a** (52 mg, 0.19 mmol) and LiOH·H_2O (48 mg, 1.1 mmol) in 10 mL of MeOH:THF:H_2O = 2:2:1 was stirred at rt for 1 h. Then, the reaction was concentrated under vacuum and acidified to pH 4−5 with 1 M aqueous HCl. The mixture was extracted with EtOAc, and the combined organic layers were washed with brine, dried over anhydrous Na_2SO_4, and concentrated to afford the crude compound 5-(*tert*-butyl)-1-pentyl-1*H*-pyrazole-3-carboxylic acid. To a solution of 5-(*tert*-butyl)-1-pentyl-1*H*-pyrazole-3- carboxylic acid (43 mg, 0.18 mmol) and 1-adamantylamine in CH_2Cl_2 (10 mL) was added HATU (82 mg, 0.22 mmol), followed by DIPEA (0.1 mL, 0.36 mmol). The mixture was stirred at rt for 5 h. Then, the reaction was concentrated under vacuum and the crude mixture was extracted with EtOAc. The combined organic layers were washed with brine, dried over anhydrous Na_2SO_4, and concentrated. The residue was purified by flash chromatography on silica gel to give the title compound **23** (40 mg, 67.5%) as a white solid. ^{1}H NMR (500 MHz, $CDCl_3$) δ 6.61 (s, 1H), 6.48 (s, 1H), 4.25−4.00 (m, 2H), 2.16−2.04 (m, 9H), 1.95−1.85 (m, 2H), 1.72−1.68 (m, 6H), 1.42−1.31 (m, 13H), 0.93 (t, J = 6.9, 3H). ^{13}C NMR (151 MHz, $CDCl_3$) δ 161.6, 152.7, 145.7, 103.5, 51.5, 51.5, 41.7 (3C), 36.5 (3C), 31.4, 30.4, 30.1 (3C), 29.5 (3C), 29.0, 22.4, 14.0. HRMS (ESI): calcd for $C_{23}H_{37}N_3NaO$ [M + Na]$^+$, 394.2834; found 394.2803. mp: 56−58 °C. HPLC purity = 95.4%; t_R = 5.2 min.

*5-(tert-Butyl)-N-(3-hydroxyadamantan-1-yl)-1-pentyl-1H-pyrazole-3-carboxamide (**24**).* The title compound was prepared by the same procedure described for **23** except using 3-amino-1-adamantanol instead of 1-adamantylamine as a white solid. ^{1}H NMR (500 MHz, $CDCl_3$) δ 6.69 (s, 1H), 6.49 (s, 1H), 4.13−4.10 (m, 2H), 2.33−2.27 (m, 2H), 2.16−2.11 (m, 2H), 1.97−1.90 (m, 2H), 1.74 (m, 4H), 1.61 (m, 6H), 1.49−1.31 (m, 13H), 0.93 (t, J = 7.0 Hz, 3H). ^{13}C NMR (101 MHz, $CDCl_3$) δ 161.5, 152.9, 145.3, 103.7, 69.3, 54.0, 51.5, 49.2, 44.2 (2C), 40.3 (2C), 35.0, 31.4, 30.7 (2C), 30.5, 30.1 (3C), 29.0, 22.4, 14.0. HRMS (ESI): calcd for $C_{23}H_{37}N_3NaO_2$ [M + Na]$^+$, 410.2783; found 410.2750. mp: 93−95 °C. HPLC purity = 97.3%; t_R = 10.5 min.

*N,5-Di-tert-butyl-1-pentyl-1H-pyrazole-3-carboxamide (**25**).* The title compound was prepared by the same procedure described for **23** except using *tert*-butylamine instead of 1-adamantylamine as a white solid. ^{1}H NMR (500 MHz, $CDCl_3$) δ 6.72 (s, 1H), 6.50 (s, 1H), 4.13−4.10 (m, 2H), 1.92−1.90 (m, 2H), 1.45 (s, 9H), 1.38−1.37 (m, 4H), 1.36 (s, 9H), 0.93 (t, J = 7.0 Hz, 3H). ^{13}C NMR (101 MHz, $CDCl_3$) δ 161.8, 152.8, 145.5, 103.6, 51.5, 50.9, 31.4, 30.5, 30.1 (3C), 29.0, 28.9 (3C), 22.4, 14.0. HRMS (ESI): calcd for $C_{17}H_{31}N_3NaO$ [M + Na]$^+$, 316.2365; found 316.2350. mp: 90−93 °C. HPLC purity = 97.6%; t_R = 10.3 min.

*5-(tert-Butyl)-N-(1-hydroxy-2-methylpropan-2-yl)-1-pentyl-1H-pyrazole-3-carboxamide (**26**).* The title compound was prepared by the same procedure described for **23** except using 2-amino-2-methyl-1-propanol instead of 1-adamantylamine as a white solid. ^{1}H NMR (500 MHz, $CDCl_3$) δ 6.91 (s, 1H), 6.51 (s, 1H), 4.14−4.11 (m, 2H), 3.67 (s, 2H), 1.94−1.88 (m, 2H), 1.38 (s, 6H), 1.37−1.34 (m, 11H), 1.27−1.23 (m, 2H), 0.93 (t, J = 6.2 Hz, 3H). ^{13}C NMR (101 MHz, $CDCl_3$) δ 163.2, 153.2, 144.3, 103.9, 71.0, 56.1, 51.6, 31.4, 30.5, 30.0 (3C), 29.0, 24.9 (2C), 22.4, 14.0. HRMS (ESI): calcd for $C_{17}H_{31}N_3NaO_2$ [M + Na]$^+$, 332.2314; found 332.2297. mp: 92−95 °C. HPLC purity = 98.5%; t_R = 6.0 min.

*5-(tert-Butyl)-1-pentyl-N-(4-chlorophenyl)-1H-pyrazole-3-carboxamide (**27**).* The title compound was prepared by the same procedure described for **23** except using 4-chloroaniline instead of 1-adamantylamine as a colorless oil. ^{1}H NMR (600 MHz, $CDCl_3$) δ 8.71 (s, 1H), 7.66 (d, J = 8.8 Hz, 2H), 7.31 (d, J = 8.8 Hz, 2H), 6.63 (s, 1H), 4.25−4.13 (m, 2H), 2.02−1.93 (m, 2H), 1.47−1.37 (m, 13H), 0.96 (t, J = 6.9 Hz, 3H). ^{13}C NMR (151 MHz, $CDCl_3$) δ 160.2, 153.5, 144.4, 136.8, 128.9 (2C), 128.6, 120.8 (2C), 104.2, 51.7, 31.5, 30.4, 30.1 (3C), 29.0, 22.4, 14.0. HRMS (ESI): calcd for $C_{19}H_{26}ClN_3NaO$ [M + Na]$^+$, 370.1662; found 370.1682. HPLC purity = 98.8%; t_R = 10.5 min.

*5-(tert-Butyl)-1-pentyl-N-(4-chlorobenzyl)-1H-pyrazole-3-carboxamide (**28**).* The title compound was prepared by the same procedure described for **23** except using 4-chlorobenzylamine instead of 1-adamantylamine as a white solid. ^{1}H NMR (500 MHz, $CDCl_3$) δ 7.28−7.26 (m, 4H), 7.17 (s, 1H), 6.56 (s, 1H), 4.57 (d, J = 6.2 Hz, 2H), 4.12−4.11 (m, 2H), 1.91−1.86 (m, 2H), 1.37 (s, 9H), 1.36−1.33 (m, 4H), 0.91 (t, J = 6.9 Hz, 3H). ^{13}C NMR (126 MHz, DMSO-d_6) δ 162.0, 152.6, 144.7, 139.5, 131.6, 129.6 (2C), 128.5 (2C), 103.8, 51.4, 41.7, 31.4, 30.6, 30.2 (3C), 28.8, 22.4, 14.3. HRMS (ESI): calcd for $C_{20}H_{28}ClN_3NaO$ [M + Na]$^+$, 384.1819; found 384.1808. mp: 136−138 °C. HPLC purity = 98.6%; t_R = 9.7 min.

*5-(tert-Butyl)-1-pentyl-N-(2-phenylpropan-2-yl)-1H-pyrazole-3-carboxamide (**29**).* The title compound was prepared by the same procedure described for **23** except using 2-phenylpropan-2-amine instead of 1-adamantylamine as a white solid. ^{1}H NMR (500 MHz, $CDCl_3$) δ 7.47−7.45 (m, 2H), 7.34−7.31 (m, 2H), 7.23−7.18 (m, 2H), 6.50 (s, 1H), 4.15−4.12 (m, 2H), 1.95−1.92 (m, 2H), 1.80 (s, 6H), 1.42−1.38 (m, 4H), 1.35 (s, 9H), 0.94 (t, J = 7.0 Hz, 3H). ^{13}C NMR (151 MHz, $CDCl_3$) δ 161.6, 152.8, 147.3, 145.3, 128.3 (2C), 126.5, 124.9 (2C), 103.8, 55.7, 51.5, 31.4, 30.5, 30.1 (3C), 29.4 (2C), 29.0, 22.4, 14.0. HRMS (ESI): calcd for $C_{22}H_{34}N_3O$ [M + H]$^+$, 356.2702; found 356.2703. mp: 138−140 °C. HPLC purity = 99.1%; t_R = 10.2 min.

*5-(tert-Butyl)-1-pentyl-N-(pyridin-4-yl)-1H-pyrazole-3-carboxamide (**30**).* The title compound was prepared by the same procedure described for **23** except using 4-aminopyridine instead of 1-adamantyl-

https://dx.doi.org/10.1021/acs.jmedchem.0c01023
J. Med. Chem. 2021, 64, 385−403

amine as a colorless oil. ^{1}H NMR (500 MHz, $CDCl_3$) δ 8.83 (s, 1H), 8.50 (d, J = 6.2 Hz, 2H), 7.63 (d, J = 6.3 Hz, 2H), 6.62 (s, 1H), 4.19−4.13 (m, 2H), 1.98−1.91 (m, 2H), 1.41−1.36 (m, 13H), 0.93 (t, J = 6.9 Hz, 3H). ^{13}C NMR (126 MHz, $CDCl_3$) δ 160.7, 153.8, 150.5 (2C), 145.2, 143.8, 113.5 (2C), 104.4, 51.8, 31.5, 30.5, 30.0 (3C), 29.0, 22.4, 14.0. HRMS (ESI): calcd for $C_{18}H_{27}N_4O$ $[M + H]^+$, 315.2185; found 315.2154. HPLC purity = 97.9%; t_R = 9.5 min.

*5-(tert-Butyl)-N-cyclohexyl-1-pentyl-1H-pyrazole-3-carboxamide (**31**).* The title compound was prepared by the same procedure described for **23** except using cyclohexane instead of 1-adamantylamine as a colorless oil. ^{1}H NMR (500 MHz, $CDCl_3$) δ 6.70 (d, J = 7.8 Hz, 1H), 6.52 (s, 1H), 4.13−4.10 (m, 2H), 3.95−3.85 (m, 1H), 1.98−1.91 (m, 2H), 1.90−1.88 (m, 2H), 1.74−1.72 (m, 2H), 1.54−1.33 (m, 15H), 1.26−1.14 (m, 4H), 0.93 (t, J = 6.8 Hz, 3H). ^{13}C NMR (126 MHz, $CDCl_3$) δ 161.4, 152.7, 144.9, 103.8, 51.5, 47.7, 33.3 (2C), 31.4, 30.5, 30.1 (3C), 29.0, 25.7, 25.0, 22.4, 14.0, 1.0. HRMS (ESI): calcd for $C_{19}H_{33}N_3NaO$ $[M + Na]^+$, 342.2521; found 342.2537. HPLC purity = 98.2%; t_R = 7.6 min.

*Methyl (R)-2-(5-(tert-Butyl)-1-pentyl-1H-pyrazole-3-carboxamido)-3,3-dimethyl-butanoate (**32**).* The title compound was prepared by the same procedure described for **23** except using methyl (*R*)-2-amino-3,3-dimethylbutanoate instead of 1-adamantylamine as a colorless oil. ^{1}H NMR (500 MHz, $CDCl_3$) δ 7.38 (d, J = 9.6 Hz, 1H), 6.52 (s, 1H), 4.63 (d, J = 9.7 Hz, 1H), 4.14 (t, J = 7.8 Hz, 2H), 3.73 (s, 3H), 1.99−1.90 (m, 2H), 1.42−1.37 (m, 4H), 1.36 (s, 9H), 1.04 (s, 9H), 0.93 (t, J = 6.5 Hz, 3H). ^{13}C NMR (101 MHz, $CDCl_3$) δ 172.1, 162.0, 152.9, 143.8, 104.1, 59.6, 51.7, 51.6, 35.0, 31.4, 30.4, 30.1 (3C), 29.0, 26.6 (3C), 22.4, 14.0. HRMS (ESI): calcd for $C_{20}H_{35}N_3NaO_3$ $[M + Na]^+$, 388.2576; found 388.2551. HPLC purity = 96.1%; t_R = 9.2 min.

*Methyl (5-(tert-Butyl)-1-pentyl-1H-pyrazole-3-carbonyl)-D-valinate (**33**).* The title compound was prepared by the same procedure described for **23** except using methyl D-valinate instead of 1-adamantylamine as a colorless oil. ^{1}H NMR (500 MHz, $CDCl_3$) δ 7.28 (s, 1H), 6.52 (s, 1H), 4.77−4.57 (m, 1H), 4.14 (t, J = 7.8 Hz, 2H), 3.75 (s, 3H), 2.28−2.20 (m, 1H), 1.98−1.85 (m, 2H), 1.43−1.31 (m, 13H), 1.03−0.96 (m, 6H), 0.93 (t, J = 6.8 Hz, 3H). ^{13}C NMR (126 MHz, $CDCl_3$) δ 172.6, 162.3, 152.8, 143.9, 103.9, 56.7, 52.1, 51.6, 31.6, 31.4, 30.4, 30.1 (3C), 29.0, 22.4, 19.1, 18.0, 14.0. HRMS (ESI): calcd for $C_{19}H_{33}N_3NaO_3$ $[M + Na]^+$, 374.2420; found 374.2395. HPLC purity = 98.0%; t_R = 8.7 min.

*Methyl (5-(tert-Butyl)-1-pentyl-1H-pyrazole-3-carbonyl)-L-valinate (**34**).* The title compound was prepared by the same procedure described for **23** except using methyl L-valinate instead of 1-adamantylamine as a colorless oil. ^{1}H NMR (500 MHz, $CDCl_3$) δ 7.28 (d, J = 9.3 Hz, 1H), 6.53 (s, 1H), 4.71 (dd, J = 9.2, 5.3 Hz, 1H), 4.14 (t, J = 7.9 Hz, 2H), 3.75 (s, 3H), 2.33−2.16 (m, 1H), 1.99−1.60 (m, 2H), 1.42−1.38 (m, 4H), 1.36 (s, 9H), 0.99 (dd, J = 10.4, 6.9 Hz, 6H), 0.94 (t, J = 7.0 Hz, 3H). ^{13}C NMR (101 MHz, $CDCl_3$) δ 172.6. 162.3, 152.9, 143.9, 104.0, 56.8, 52.0, 51.6, 31.5, 31.4, 30.4, 30.1 (3C), 29.0, 22.4, 19.1, 18.0, 14.0. HRMS (ESI): calcd for $C_{19}H_{33}N_3NaO_3$ $[M + Na]^+$, 374.2420; found 374.2389. HPLC purity = 96.2%; t_R = 10.5 min.

*N-(1-Hydroxy-2-methylpropan-2-yl)-1-pentyl-5-(trifluoromethyl)-1H-pyrazole-3-carboxamide (**35**).* The title compound was prepared by the same procedure described for **26** except using 1,1,1-trifluoroacetone instead of 3,3-dimethyl-2-butanone as a colorless oil. ^{1}H NMR (500 MHz, $CDCl_3$) δ 7.07 (s, 1H), 6.88 (s, 1H), 4.18 (t, J = 7.5 Hz, 2H), 3.69 (s, 2H), 1.92−1.87 (m, 2H), 1.40 (s, 6H), 1.38−1.30 (m, 4H), 0.91 (t, J = 7.0 Hz, 3H). ^{13}C NMR (126 MHz, $CDCl_3$) δ 161.3, 145.6, 137.0−129.9, 119.6, 108.1, 70.5, 56.3, 51.9, 29.8, 28.5, 24.8, 22.1, 13.8, 1.0. HRMS (ESI): calcd for $C_{14}H_{22}F_3N_3NaO_2$ $[M + Na]^+$, 344.1562; found 344.1578. HPLC purity = 97.8%; t_R = 5.0 min.

*N-(1-Hydroxy-2-methylpropan-2-yl)-5-isopropyl-1-pentyl-1H-pyrazole-3-carboxamide (**36**).* The title compound was prepared by the same procedure described for **26** except using 3-methyl-2-butanone instead of 3,3-dimethyl-2-butanone as a light yellow solid. ^{1}H NMR (500 MHz, $CDCl_3$) δ 6.93 (s, 1H), 6.54 (s, 1H), 5.27 (s, 1H), 4.00 (t, J = 7.5 Hz, 2H), 3.67 (s, 2H), 2.96−2.86 (m, 1H), 1.88−1.80 (m, 2H), 1.38 (s, 6H), 1.37−1.28 (m, 4H), 1.25 (d, J = 6.8 Hz, 6H), 0.92 (t, J = 7.1 Hz, 3H). ^{13}C NMR (101 MHz, $CDCl_3$) δ 163.2, 151.3, 145.1, 102.6, 71.0, 56.1, 49.3, 30.2, 28.8, 25.4, 24.9 (2C), 22.8 (2C), 22.3, 13.9. HRMS (ESI): calcd for $C_{16}H_{29}N_3NaO_2$ $[M + Na]^+$, 318.2157; found 318.2134. mp: 37−38 °C. HPLC purity = 97.4%; t_R = 7.3 min.

*N-(1-Hydroxy-2-methylpropan-2-yl)-5-neopentyl-1-pentyl-1H-pyrazole-3-carboxamide (**37**).* The title compound was prepared by the same procedure described for **26** except using 4,4-dimethyl-2-pentanone instead of 3,3-dimethyl-2-butanone as a white solid. ^{1}H NMR (500 MHz, $CDCl_3$) δ 6.96 (s, 1H), 6.54 (s, 1H), 4.03−3.99 (m, 2H), 3.68 (s, 2H), 2.51 (s, 2H), 1.86−1.79 (m, 2H), 1.39 (s, 6H), 1.38−1.33 (m, 2H), 1.32−1.27 (m, 2H), 0.95 (s, 9H), 0.91 (t, J = 7.2 Hz, 3H). ^{13}C NMR (101 MHz, $CDCl_3$) δ 163.2, 144.8, 142.5, 106.8, 70.9, 56.1, 49.6, 39.0, 32.1, 20.0, 29.4 (3C), 28.8, 24.9 (2C), 22.3, 13.9. HRMS (ESI): calcd for $C_{18}H_{33}N_3NaO_2$ $[M + Na]^+$, 346.2470; found 346.2442. mp: 46−48 °C. HPLC purity = 98.9%; t_R = 4.2 min.

*5-Cyclopropyl-I-N-(1-hydroxy-2-methylpropan-2-yl)-1-pentyl-1H-pyrazole-3-carboxamide (**38**).* The title compound was prepared by the same procedure described for **26** except using cyclopropylmethyl ketone instead of 3,3-dimethyl-2-butanone as a light yellow solid. ^{1}H NMR (500 MHz, $CDCl_3$) δ 6.91 (s, 1H), 6.32 (s, 1H), 4.16−4.13 (m, 2H), 3.66 (s, 2H), 1.90−1.83 (m, 2H), 1.73−1.68 (m, 1H), 1.38 (s, 6H), 1.36−1.28 (m, 4H), 1.03−0.96 (m, 2H), 0.92 (t, J = 7.1 Hz, 3H), 0.72−0.54 (m, 3H). ^{13}C NMR (101 MHz, $CDCl_3$) δ 163.1, 147.0, 144.8, 103.0, 71.0, 56.2, 49.7, 29.8, 28.8, 25.0 (2C), 22.3, 13.9, 7.3 (2C), 6.1. HRMS (ESI): calcd for $C_{16}H_{27}N_3NaO_2$ $[M + Na]^+$, 316.2001; found 316.1989. mp: 45−48 °C. HPLC purity = 98.9%; t_R = 4.2 min.

*5-Cyclohexyl-N-(1-hydroxy-2-methylpropan-2-yl)-1-pentyl-1H-pyrazole-3-carboxamide (**39**).* The title compound was prepared by the same procedure described for **26** except using 1-cyclohexylethanone instead of 3,3-dimethyl-2-butanone as a white solid. ^{1}H NMR (500 MHz, $CDCl_3$) δ 6.92 (s, 1H), 6.51 (s, 1H), 4.00−3.98 (m, 2H), 3.67 (s, 2H), 2.51 (t, J = 9.0 Hz, 1H), 1.85−1.82 (m, 6H), 1.38−1.30 (m, 16H), 0.92 (t, J = 7.1 Hz, 3H). ^{13}C NMR (101 MHz, $CDCl_3$) δ 163.1, 150.4, 145.0, 103.1, 71.1, 56.2, 49.3, 35.3, 33.2 (2C), 30.2, 28.8, 26.3 (2C), 25.7, 25.0 (2C), 22.3, 13.93. HRMS (ESI): calcd for $C_{19}H_{33}N_3NaO_2$ $[M + Na]^+$, 358.2470; found 358.2469. mp: 84−86 °C. HPLC purity = 97.7%; t_R = 6.0 min.

*5-(2,4-Difluorophenyl)-N-(1-hydroxy-2-methylpropan-2-yl)-1-pentyl-1H-pyrazole-3-carboxamide (**40**).* The title compound was prepared by the same procedure described for **26** except using 2′,4′-difluoroacetophenone instead of 3,3-dimethyl-2-butanone as a white solid. ^{1}H NMR (500 MHz, $CDCl_3$) δ 7.31−7.28 (m, 1H), 6.99−6.94 (m, 3H), 6.77 (s, 1H), 3.96 (t, J = 7.4 Hz, 2H), 3.71 (s, 2H), 1.80−1.74 (m, 2H), 1.42 (s, 6H), 1.18−1.12 (m, 2H), 1.19−1.11 (m, 2H), 0.83 (t, J = 7.2 Hz, 3H). ^{13}C NMR (101 MHz, $CDCl_3$) δ 162.6, 145.8, 138.1, 132.6, 114.2, 112.0, 108.1, 104.7, 70.8, 56.2, 50.3, 29.6, 28.5, 24.9 (2C), 24.8 (2C), 22.0, 13.8. HRMS (ESI): calcd for $C_{19}H_{25}F_2N_3NaO_2$ $[M + Na]^+$, 388.1813; found 388.1786. mp: 85−88 °C. HPLC purity = 96.2%; t_R = 6.0 min.

*5-(tert-Butyl)-4-chloro-N-(1-hydroxy-2-methylpropan-2-yl)-1-pentyl-1H-pyrazole-3-carboxamide (**41**).* To a solution of **26** (1.878 g, 5.7 mmol) and NCS (837 mg, 6.3 mmol) in $CHCl_3$ (20 mL) was slowly added dibenzoyl peroxide (138 mg, 0.57 mmol). The mixture was refluxed overnight. Then, the reaction was concentrated under vacuum and the crude mixture was extracted with EtOAc. The combined organic layers were washed with brine, dried over anhydrous Na_2SO_4, and concentrated. The residue was purified by flash chromatography on silica gel to give the title compound **41** (1.190 g, 69.4%) as a white solid. ^{1}H NMR (500 MHz, $CDCl_3$) δ 6.88 (s, 1H), 4.23−4.20 (m, 2H), 3.68 (s, 2H), 1.90−1.75 (m, 2H), 1.51 (s, 9H), 1.40−1.30 (m, 10H), 0.92 (t, J=7.0, 3H). ^{13}C NMR (101 MHz, $CDCl_3$) δ 162.0, 146.3, 140.2, 108.0, 70.7, 56.3, 53.7, 33.7, 30.8, 30.2 (3C), 28.7, 24.9 (2C), 22.3, 14.0. HRMS (ESI): calcd for $C_{17}H_{30}ClN_3NaO_2$ $[M + Na]^+$, 366.1924; found 366.1941. mp: 82−84 °C. HPLC purity = 95.3%; t_R = 9.3 min.

*4-Bromo-5-(tert-butyl)-N-(1-hydroxy-2-methylpropan-2-yl)-1-pentyl-1H-pyrazole-3-carboxamide (**42**).* The title compound was prepared by the same procedure described for **41** except using NBS instead of NCS as a yellow solid. ^{1}H NMR (500 MHz, $CDCl_3$) δ 6.90 (s, 1H), 4.29−4.21 (m, 2H), 3.69 (s, 2H), 1.89−1.80 (m, 2H), 1.53−1.47 (m, 9H), 1.43−1.30 (m, 10H), 0.93 (t, J = 7.0 Hz, 3H). ^{13}C NMR (101

https://dx.doi.org/10.1021/acs.jmedchem.0c01023
J. Med. Chem. 2021, 64, 385−403

MHz, $CDCl_3$) δ 162.2, 147.4, 141.5, 91.8, 70.7, 56.2, 54.1, 34.0, 31.0, 30.5 (3C), 28.7, 24.9 (2C), 22.3, 14.0. HRMS (ESI): calcd for $C_{17}H_{30}BrN_3NaO_2$ $[M + Na]^+$, 410.1419; found 410.1401. mp: 87−88 °C. HPLC purity = 97.4%; t_R = 8.7 min.

*5-(tert-Butyl)-N-(1-hydroxy-2-methylpropan-2-yl)-4-nitro-1-pentyl-1H-pyrazole-3-carboxamide (**43**).* To a solution of **26** (279 mg, 0.9 mmol) in $CHCl_3$ (10 mL) was added copper dinitrate (253 mg, 1.3 mmol). Then, TFAA (1.3 mL, 9.0 mmol) was gradually added. The mixture was stirred at rt overnight. Then, the reaction was concentrated under vacuum and the crude mixture was extracted with EtOAc. The combined organic layers were washed with brine, dried over anhydrous Na_2SO_4, and concentrated. The residue was purified by flash chromatography on silica gel to give the title compound **43** (225 g, 70.5%) as a yellow solid. ^{1}H NMR (500 MHz, $CDCl_3$) δ 6.69 (s, 1H), 4.17−4.13 (m, 2H), 3.67 (s, 2H), 1.99−1.85 (m, 2H), 1.60−1.25 (m, 19H), 0.95 (t, J = 6.8 Hz, 3H). ^{13}C NMR (101 MHz, $CDCl_3$) δ 159.6, 143.6, 136.3, 132.1, 70.1, 56.4, 52.9, 33.3, 30.2, 28.8 (3C), 28.8 (2C), 24.8, 22.3, 13.9. HRMS (ESI): calcd for $C_{17}H_{30}N_4NaO_4$ $[M + Na]^+$, 377.2165; found 377.2179. mp: 92−95 °C. HPLC purity = 97.5%; t_R = 5.2 min.

*4-Amino-5-(tert-butyl)-N-(1-hydroxy-2-methylpropan-2-yl)-1-pentyl-1H-pyrazole-3-carboxamide (**44**).* To a solution of **43** (100 mg, 0.3 mmol) in MeOH (10 mL) and 3N HCl (10 mL) was slowly added zinc powder (1.961 g, 30.0 mmol) with ice cooling. The mixture was stirred at rt for 1 h. The resulting mixture was filtered through a pad of diatomaceous earth and washed with MeOH. The filtrate was concentrated under vacuum, and the crude mixture was extracted with EtOAc. The combined organic layers were washed with brine, dried over anhydrous Na_2SO_4, and concentrated. The residue was purified by flash chromatography on silica gel to give the title compound **44** (41 mg, 42.8%) as a colorless oil. ^{1}H NMR (500 MHz, $CDCl_3$) δ 6.80 (s, 1H), 4.12−3.99 (m, 2H), 3.65 (s, 2H), 1.94−1.78 (m, 2H), 1.45 (s, 9H), 1.41−1.31 (m, 10H), 0.92 (t, J = 6.9 Hz, 3H). ^{13}C NMR (101 MHz, $CDCl_3$) δ 165.3, 134.8, 131.6, 128.6, 71.1, 56.0, 52.4, 32.9, 30.5, 30.4 (3C), 28.9, 25.0 (2C), 22.4, 14.0. HRMS (ESI): calcd for $C_{17}H_{32}N_4NaO_2$ $[M + Na]^+$, 347.2423; found 347.2404. HPLC purity = 97.8%; t_R = 5.3 min.

*5-(tert-Butyl)-N-(1-hydroxy-2-methylpropan-2-yl)-1-propyl-1H-pyrazole-3-carboxamide (**45**).* The title compound was prepared by the same procedure described for **26** except using 1-bromopropane instead of 1-bromopentane as a white solid. ^{1}H NMR (500 MHz, $CDCl_3$) δ 6.92 (s, 1H), 6.52 (s, 1H), 4.11−4.08 (m, 2H), 3.67 (s, 2H), 1.98−1.91 (m, 2H), 1.38 (s, 6H), 1.36 (s, 9H), 0.99 (t, J = 7.4 Hz, 3H). ^{13}C NMR (126 MHz, $CDCl_3$) δ 163.2, 153.3, 144.3, 103.9, 71.0, 56.2, 53.1, 31.4, 30.1 (3C), 25.0 (2C), 24.0, 11.2. HRMS (ESI): calcd for $C_{15}H_{27}N_3NaO_2$ $[M + Na]^+$, 304.2001; found 304.1987. mp: 58−60 °C. HPLC purity = 96.9%; t_R = 9.5 min.

*5-(tert-Butyl)-1-butyl-N-(1-hydroxy-2-methylpropan-2-yl)-1H-pyrazole-3-carboxamide (**46**).* The title compound was prepared by the same procedure described for **26** except using 1-bromobutane instead of 1-bromopentane as a white solid. ^{1}H NMR (500 MHz, $CDCl_3$) δ 6.91 (s, 1H), 6.52 (s, 1H), 4.15−4.12 (m, 2H), 3.67 (s, 2H), 1.92−1.88 (m, 2H), 1.46−1.41 (m, 2H), 1.38 (s, 6H), 1.37 (s, 9H), 0.99 (t, J = 7.4 Hz, 3H). ^{13}C NMR (101 MHz, $CDCl_3$) δ 163.2, 153.2, 144.4, 103.9, 71.0, 56.1, 51.4, 32.8, 31.4 (3C), 30.1 (2C), 25.0, 20.1, 13.8. HRMS (ESI): calcd for $C_{16}H_{29}N_3NaO_2$ $[M + Na]^+$, 318.2157; found 318.2135. mp: 81−83 °C. HPLC purity = 97.2%; t_R = 9.3 min.

*5-(tert-Butyl)-1-hexyl-N-(1-hydroxy-2-methylpropan-2-yl)-1H-pyrazole-3-carboxamide (**47**).* The title compound was prepared by the same procedure described for **26** except using 1-bromohexane instead of 1-bromopentane as a white solid. ^{1}H NMR (500 MHz, $CDCl_3$) δ 6.95 (s, 1H), 6.52 (s, 1H), 4.15−4.12 (m, 2H), 3.67 (s, 2H), 1.94−1.90 (m, 2H), 1.43−1.39 (s, 8H), 1.36 (s, 9H), 1.34−1.33 (m, 4H), 0.91 (t, J = 7.0 Hz, 3H). ^{13}C NMR (101 MHz, $CDCl_3$) δ 163.1, 153.2, 144.3, 104.0, 71.1, 56.2, 51.6, 31.4, 31.4, 30.7, 30.1 (3C), 26.5, 25.0 (2C), 22.5, 14.0. HRMS (ESI): calcd for $C_{18}H_{33}N_3NaO_2$ $[M + Na]^+$, 346.2470; found 346.2466. mp: 88−90 °C. HPLC purity = 96.0%; t_R = 10.3 min.

*5-(tert-Butyl)-1-(3-fluoropropyl)-N-(1-hydroxy-2-methylpropan-2-yl)-1H-pyrazole-3-carboxamide (**48**).* The title compound was prepared by the same procedure described for **26** except using 1-bromo-3-fluoropropane instead of 1-bromopentane as a white solid. ^{1}H NMR (500 MHz, $CDCl_3$) δ 6.93 (s, 1H), 6.55 (s, 1H), 4.61 (t, J = 5.5 Hz, 1H), 4.51 (t, J = 5.5 Hz, 1H), 4.37−4.32 (m, 2H), 3.67 (s, 2H), 2.42−2.37 (m, 1H), 2.35−2.30 (m, 1H), 1.38 (s, 15H). ^{13}C NMR (101 MHz, $CDCl_3$) δ 162.9, 153.9, 144.8, 104.1, 81.9−80.2, 70.9, 56.1, 47.6, 31.4, 31.3, 29.9 (3C), 24.9 (2C). HRMS (ESI): calcd for $C_{15}H_{26}FN_3NaO_2$ $[M + Na]^+$, 322.1907; found 322.1893. mp: 81−83 °C. HPLC purity = 99.7%; t_R = 2.9 min.

*5-(tert-Butyl)-1-(4-fluorobutyl)-N-(1-hydroxy-2-methylpropan-2-yl)-1H-pyrazole-3-carboxamide (**49**).* The title compound was prepared by the same procedure described for **26** except using 1-bromo-4-fluorobutane instead of 1-bromopentane as a white solid. ^{1}H NMR (500 MHz, $CDCl_3$) δ 6.90 (s, 1H), 6.53 (s, 1H), 4.56 (t, J = 5.8 Hz, 1H), 4.47 (t, J = 5.8 Hz, 1H), 4.22−4.19 (m, 2H), 3.67 (s, 2H), 2.10−2.05 (m, 2H), 1.86−1.78 (m, 2H), 1.38 (s, 6H), 1.37 (s, 9H). ^{13}C NMR (101 MHz, $CDCl_3$) δ 163.1, 153.4, 144.5, 104.0, 84.5−82.8, 71.0, 56.2, 51.0, 31.4, 30.0 (3C), 27.7, 26.9, 25.0 (2C). HRMS (ESI): calcd for $C_{16}H_{28}FN_3NaO_2$ $[M + Na]^+$, 336.2063; found 336.2034. mp: 97−98 °C. HPLC purity = 99.1%; t_R = 3.1 min.

*5-(tert-Butyl)-1-(5-fluoropentyl)-N-(1-hydroxy-2-methylpropan-2-yl)-1H-pyrazole-3-carboxamide (**50**).* The title compound was prepared by the same procedure described for **26** except using 1-bromo-5-fluoropentane instead of 1-bromopentane as a yellow solid. ^{1}H NMR (500 MHz, DMSO-d_6) δ 7.06 (s, 1H), 6.31 (s, 1H), 5.08 (s, 1H), 4.49 (t, J = 6.0 Hz, 1H), 4.41 (t, J = 6.0 Hz, 1H), 4.17−4.14 (m, 2H), 3.40 (d, J = 5.6 Hz, 2H), 1.88−1.82 (m, 2H), 1.74−1.66 (m, 2H), 1.48−1.42 (m, 2H), 1.33 (s, 9H), 1.29 (s, 6H). ^{13}C NMR (101 MHz, $CDCl_3$) δ 162.7, 153.7, 144.0, 104.4, 84.5−82.9, 70.8, 56.3, 51.4, 39.0, 31.5, 30.0 (3C), 30.0, 24.8 (2C), 22.6. HRMS (ESI): calcd for $C_{17}H_{30}FN_3NaO_2$ $[M + Na]^+$, 350.2220; found 350.2235. mp: 161−163 °C. HPLC purity = 97.1%; t_R = 9.5 min.

*5-(tert-Butyl)-1-(cyclopropylmethyl)-N-(1-hydroxy-2-methylpropan-2-yl)-1H-pyrazole-3-carboxamide (**51**).* The title compound was prepared by the same procedure described for **26** except using (bromomethyl)cyclopropane instead of 1-bromopentane as a white solid. ^{1}H NMR (400 MHz, $CDCl_3$) δ 6.94 (s, 1H), 6.54 (s, 1H), 4.05 (d, J = 6.8 Hz, 2H), 3.67 (s, 2H), 1.38 (s, 6H), 1.37 (s, 9H), 1.29−1.27 (m, 1H), 0.66−0.58 (m, 2H), 0.48−0.40 (m, 2H). ^{13}C NMR (101 MHz, $CDCl_3$) δ 163.2, 153.2, 144.4, 104.0, 71.0, 56.1, 55.7, 31.5, 30.2 (3C), 25.0 (2C), 11.6, 4.1 (2C). HRMS (ESI): calcd for $C_{16}H_{27}N_3NaO_2$ $[M + Na]^+$, 316.2001. found 316.1985. HPLC purity = 95.6%; t_R = 9.5 min.

*5-(tert-Butyl)-N-(1-hydroxy-2-methylpropan-2-yl)-1-(2-methoxyethyl)-1H-pyrazole-3-carboxamide (**52**).* The title compound was prepared by the same procedure described for **26** except using 1-bromo-2-methoxyethane instead of 1-bromopentane. ^{1}H NMR (500 MHz, $CDCl_3$) δ 6.84 (s, 1H), 6.38 (s, 1H), 4.54 (t, J = 5.5 Hz, 2H), 3.78 (t, J = 4.9 Hz, 2H), 3.69 (s, 2H), 3.33 (s, 3H), 1.37 (s, 6H), 1.29 (s, 9H). ^{13}C NMR (126 MHz, $CDCl_3$) δ 163.0, 154.1, 144.8, 104.1, 71.0, 59.2, 56.1, 50.8, 38.6, 31.4, 30.0 (3C), 24.9 (2C). HRMS (ESI): calcd for $C_{15}H_{27}N_3NaO_3$ $[M + Na]^+$, 320.1950; found 320.1959. mp: 64−66 °C. HPLC purity = 96.5%; t_R = 9.2 min.

General Synthetic Procedure of *N*-Aryl-Substituted Pyrazoles. *Ethyl 5-(tert-Butyl)-1-phenyl-1H-pyrazole-3-carboxylate (**53a**).* To a solution of 3,3-dimethyl-2-butanone (1002 mg, 10.0 mmol) in anhydrous THF (250 mL) was added *t*-BuOK (1459 mg, 13.0 mmol) with ice cooling. After stirring for 10 min, diethyl oxalate (1.36 mL, 10.0 mmol) was added. The reaction mixture was refluxed for 5 h. Then, phenylhydrazine hydrochloride (1591 mg, 11.0 mmol) was added dropwise to the mixture, followed by the addition of acetic acid (1.5 mL). The mixture was stirred at 60 °C for 3 h. Then, the reaction was concentrated under vacuum and the crude mixture was extracted with EtOAc. The combined organic layers were washed with brine, dried over anhydrous Na_2SO_4, and concentrated. The residue was purified by flash chromatography on silica gel to give the title compound **53a** (2.350 g, 86.2%). ^{1}H NMR (400 MHz, $CDCl_3$) δ 7.48−7.35 (m, 5H), 6.74 (s, 1H), 4.39 (d, J = 6.8 Hz, 2H), 1.37 (t, J = 6.6 Hz, 3H), 1.18 (s, 9H). LRMS (ESI): calcd for $C_{16}H_{20}N_2O_2$, 272.15; found 272.

https://dx.doi.org/10.1021/acs.jmedchem.0c01023
J. Med. Chem. 2021, 64, 385−403

*5-(tert-Butyl)-1-phenyl-N-(1-hydroxy-2-methylpropan-2-yl)-1H-pyrazole-3-carboxamide (**54**).* A solution of **53a** (254 mg, 1.1 mmol) and LiOH·H_2O (240 mg, 5.7 mmol) in 10 mL of MeOH:THF:H_2O = 2:2:1 was stirred at rt for 1 h. Then, the reaction was concentrated under vacuum and acidified to pH 4−5 with 1 M aqueous HCl. The mixture was extracted with EtOAc, and the combined organic layers were washed with brine, dried over anhydrous Na_2SO_4, and concentrated to afford the crude compound 5-(*tert*-butyl)-1-phenyl-1*H*-pyrazole-3-carboxylic acid. To a solution of 5-(*tert*-butyl)-1-phenyl-1*H*-pyrazole-3-carboxylic acid (215 mg, 1.1 mmol) and 2-amino-2-methylpropan-1-ol (0.11 mL, 1.1 mmol) in CH_2Cl_2 (10 mL) was added HATU (521 mg, 1.4 mmol), followed by DIPEA (0.40 mL, 2.3 mmol). The mixture was stirred at rt for 5 h. Then, the reaction was concentrated under vacuum and the crude mixture was extracted with EtOAc. The combined organic layers were washed with brine, dried over anhydrous Na_2SO_4, and concentrated. The residue was purified by flash chromatography on silica gel to give the title compound **54** (253 mg, 72.8%) as a white solid. ^{1}H NMR (500 MHz, $CDCl_3$) δ 7.55−7.49 (m, 3H), 7.39 (d, J = 7.1 Hz, 2H), 6.97 (s, 1H), 6.74 (s, 1H), 3.67 (s, 2H), 1.35 (s, 6H), 1.18 (s, 9H). ^{13}C NMR (126 MHz, $CDCl_3$) δ 163.0, 155.6, 145.4, 141.5, 129.8, 128.9 (2C), 128.5 (2C), 104.7, 70.9, 56.3, 32.2, 30.6 (3C), 24.9 (2C). HRMS (ESI): calcd for $C_{18}H_{25}N_3NaO_2$ $[M + Na]^+$, 338.1844; found 338.1833. mp: 180−182 °C. HPLC purity = 98.1%; t_R = 3.9 min.

*5-(tert-Butyl)-1-(p-tolyl)-N-(1-hydroxy-2-methylpropan-2-yl)-1H-pyrazole-3-carboxamide (**55**).* The title compound was prepared by the same procedure described for **54** except using 4-methylphenylhydrazine hydrochloride instead of phenylhydrazine hydrochloride as a light yellow solid. ^{1}H NMR (500 MHz, DMSO-d_6) δ 7.35−7.31 (m, 4H), 7.09 (s, 1H), 6.55 (s, 1H), 5.00 (t, J = 5.6 Hz, 1H), 3.38 (d, J = 5.6 Hz, 2H), 2.41 (s, 3H), 1.29 (s, 6H), 1.13 (s, 9H). ^{13}C NMR (151 MHz, $CDCl_3$) δ 163.1, 155.6, 145.4, 139.9, 139.0, 129.4 (2C), 128.23 (2C), 104.6, 70.9, 56.3, 32.2, 30.6 (3C), 24.9 (2C), 21.3. HRMS (ESI): calcd for $C_{19}H_{28}N_3O_2$ $[M + H]^+$, 330.2182; found 330.2180. mp: 180−182 °C. HPLC purity = 96.0%; t_R = 8.5 min.

*5-(tert-Butyl)-1-(4-fluorophenyl)-N-(1-hydroxy-2-methylpropan-2-yl)-1H-pyrazole-3-carboxamide (**56**).* The title compound was prepared by the same procedure described for **54** except using (4-fluorophenyl)hydrazine hydrochloride instead of phenylhydrazine hydrochloride as a white solid. ^{1}H NMR (500 MHz, $CDCl_3$) δ 7.37−7.34 (m, 2H), 7.21−7.15 (m, 2H), 6.88 (s, 1H), 6.72 (s, 1H), 5.08 (s, 1H), 3.67 (s, 2H), 1.35 (s, 6H), 1.18 (s, 9H). ^{13}C NMR (151 MHz, $CDCl_3$) δ 163.8, 162.8, 162.2, 155.8, 145.7, 137.6, 130.4, 130.4, 115.9, 115.8, 104.9, 70.8, 56.3, 32.2, 30.6 (3C), 24.9 (2C). HRMS (ESI): calcd for $C_{18}H_{25}FN_3O_2$ $[M + H]^+$, 334.1931; found 334.1927. mp: 181−184 °C. HPLC purity = 99.2%; t_R = 8.4 min.

*5-(tert-Butyl)-1-(4-chlorophenyl)-N-(1-hydroxy-2-methylpropan-2-yl)-1H-pyrazole-3-carboxamide (**57**).* The title compound was prepared by the same procedure described for **54** except using 4-chlorophenylhydrazine hydrochloride instead of phenylhydrazine hydrochloride as a yellow solid. ^{1}H NMR (500 MHz, $CDCl_3$) δ 7.47 (d, J = 8.6 Hz, 2H), 7.33 (d, J = 8.6 Hz, 2H), 6.88 (s, 1H), 6.73 (s, 1H), 5.05 (s, 1H), 3.67 (s, 2H), 1.35 (s, 6H), 1.18 (s, 9H). ^{13}C NMR (151 MHz, $CDCl_3$) δ 162.8, 155.8, 145.8, 140.1, 135.8, 129.9 (2C), 129.1 (2C), 105.0, 70.8, 56.3, 32.2, 30.6 (3C), 24.9 (2C). HRMS (ESI): calcd for $C_{18}H_{25}ClN_3O_2$ $[M + H]^+$, 350.1635; found 350.1634. mp: 245−248 °C. HPLC purity = 95.2%; t_R = 8.6 min.

*5-(tert-Butyl)-1-(4-(trifluoromethyl)phenyl)-N-(1-hydroxy-2-methylpropan-2-yl)-1H-pyrazole-3-carboxamide (**58**).* The title compound was prepared by the same procedure described for **54** except using 4-(trifluoromethyl)phenylhydrazine hydrochloride instead of phenylhydrazine hydrochloride as a yellow solid. ^{1}H NMR (500 MHz, DMSO-d_6) δ 7.93 (d, J = 8.2 Hz, 2H), 7.75 (d, J = 8.2 Hz, 2H), 7.15 (s, 1H), 6.62 (s, 1H), 5.05 (t, J = 5.5 Hz, 1H), 3.37 (d, J = 5.5 Hz, 2H), 1.29 (s, 6H), 1.14 (s, 9H). ^{13}C NMR (151 MHz, $CDCl_3$) δ 162.6, 155.9, 146.1, 144.6, 132.1, 131.9, 129.1 (2C), 126.1, 126.1, 105.2, 70.8, 56.3, 32.2, 30.7 (3C), 24.9 (2C). HRMS (ESI): calcd for $C_{19}H_{25}F_3N_3O_2$ $[M + H]^+$, 384.1899; found 384.1900. mp: 247−249 °C. HPLC purity = 97.1%; t_R = 8.5 min.

*5-(tert-Butyl)-1-(4-methoxyphenyl)-N-(1-hydroxy-2-methylpropan-2-yl)-1H-pyrazole-3-carboxamide (**59**).* The title compound was prepared by the same procedure described for **54** except using (4-methoxyphenyl)hydrazine hydrochloride instead of phenylhydrazine hydrochloride as a yellow solid. ^{1}H NMR (500 MHz, $CDCl_3$) δ 7.31−7.30 (m, 2H), 7.03−6.97 (m, 2H), 6.92 (s, 1H), 6.71 (s, 1H), 3.88 (s, 3H), 3.67 (s, 2H), 1.35 (s, 6H), 1.18 (s, 9H). ^{13}C NMR (151 MHz, $CDCl_3$) δ 163.0, 160.4, 155.7, 145.3, 134.2, 129.6 (2C), 113.9 (2C), 104.6, 70.8, 56.3, 55.6, 32.1, 30.6 (3C), 24.9 (2C). HRMS (ESI): calcd for $C_{19}H_{28}N_3O_3$ $[M + H]^+$, 346.2131; found 346.2156. mp: 207−210 °C. HPLC purity = 97.7%; t_R = 8.4 min.

*5-(tert-Butyl)-1-(4-(trifluoromethoxy)phenyl)-N-(1-hydroxy-2-methylpropan-2-yl)-1H-pyrazole-3-carboxamide (**60**).* The title compound was prepared by the same procedure described for **54** except using 4-((trifluoromethoxy)phenyl)hydrazine hydrochloride instead of phenylhydrazine hydrochloride as a yellow solid. ^{1}H NMR (500 MHz, $CDCl_3$) δ 7.43−7.37 (m, 2H), 7.34−7.32 (m, 2H), 6.87 (s, 1H), 6.74 (s, 1H), 5.03 (s, 1H), 3.68 (s, 2H), 1.36 (s, 6H), 1.19 (s, 9H). ^{13}C NMR (151 MHz, $CDCl_3$) δ 162.7, 155.8, 149.9, 145.9, 139.9, 130.2 (2C), 121.1 (2C), 105.0 (2C), 70.8, 56.4, 32.2, 30.6(3C), 24.9 (2C). HRMS (ESI): calcd for $C_{19}H_{25}F_3N_3O_3$ $[M + H]^+$, 400.1848; found 400.1874. mp: 196−198 °C. HPLC purity = 98.1%; t_R = 8.6 min.

*5-(tert-Butyl)-1-(2,4-difluorophenyl)-N-(1-hydroxy-2-methylpropan-2-yl)-1H-pyrazole-3-carboxamide (**61**).* The title compound was prepared by the same procedure described for **54** except using 4-(2,4-difluorophenyl)hydrazine hydrochloride instead of phenylhydrazine hydrochloride as a yellow solid. ^{1}H NMR (600 MHz, $CDCl_3$) δ 7.43−7.39 (m, 1H), 7.04−6.97 (m, 2H), 6.86 (s, 1H), 6.70 (s, 1H), 4.96 (s, 1H), 3.66 (s, 2H), 1.35 (s, 6H), 1.18 (s, 9H). ^{13}C NMR (151 MHz, $CDCl_3$) δ 162.6, 156.5, 146.7, 131.7, 131.6, 111.6, 111.5, 105.3, 105.1, 105.0, 70.8, 56.3, 32.0, 30.0 (3C), 24.9 (2C). HRMS (ESI): calcd for $C_{18}H_{24}F_2N_3O_2$ $[M + H]^+$, 352.1837; found 352.1838. mp: 247−249 °C. HPLC purity = 98.1%; t_R = 8.3 min.

*5-(tert-Butyl)-N-(1-hydroxy-2-methylpropan-2-yl)-1-(pyridin-2-yl)-1H-pyrazole-3-carboxamide (**62**).* The title compound was prepared by the same procedure described for **54** except using 2-hydrazinylpyridine hydrochloride instead of phenylhydrazine hydrochloride as a white solid. ^{1}H NMR (500 MHz, $CDCl_3$) δ 8.59 (s, 1H), 7.95−7.88 (m, 1H), 7.52−7.41 (m, 2H), 6.96 (s, 1H), 6.76 (s, 1H), 3.66 (s, 2H), 1.35 (s, 6H), 1.25 (s, 9H). ^{13}C NMR (101 MHz, $CDCl_3$) δ 162.8, 155.9, 154.0, 148.3, 146.2, 138.6, 124.4, 122.1, 105.5, 70.8, 56.3, 32.5, 30.5 (3C), 24.9 (2C). HRMS (ESI): calcd for $C_{17}H_{24}N_4NaO_2$ $[M + Na]^+$, 339.1797; found 339.1765. mp: 138−140 °C. HPLC purity = 98.9%; t_R = 9.2 min.

*5-(tert-Butyl)-N-(1-hydroxy-2-methylpropan-2-yl)-1-(pyridin-3-yl)-1H-pyrazole-3-carboxamide (**63**).* The title compound was prepared by the same procedure described for **54** except using 3-hydrazinylpyridine hydrochloride instead of phenylhydrazine hydrochloride as a white solid. ^{1}H NMR (500 MHz, $CDCl_3$) δ 8.78 (s, 1H), 8.68 (s, 1H), 7.77 (d, J = 7.3 Hz, 1H), 7.51 (d, J = 6.6 Hz, 1H), 6.88 (s, 1H), 6.77 (s, 1H), 3.68 (s, 2H), 1.36 (s, 6H), 1.19 (s, 9H). ^{13}C NMR (101 MHz, $CDCl_3$) δ 162.6, 156.4, 150.3, 148.9, 146.4, 138.4, 136.3, 123.7, 105.2, 70.7, 56.3, 32.2, 30.7 (3C), 24.8 (2C). HRMS (ESI): calcd for $C_{17}H_{24}N_4NaO_2$ $[M + Na]^+$, 339.1797; found 339.1765. mp: 108−110 °C. HPLC purity = 97.8%; t_R = 9.0 min.

*5-(tert-Butyl)-1-(5-fluoropyridin-2-yl)-N-(1-hydroxy-2-methylpropan-2-yl)-1H-pyrazole-3-carboxamide (**64**).* The title compound was prepared by the same procedure described for **54** except using 5-fluoro-2-hydrazinylpyridine hydrochloride instead of phenylhydrazine hydrochloride as a white solid. ^{1}H NMR (500 MHz, $CDCl_3$) δ 8.42 (s, 1H), 7.64−7.59 (m, 1H), 7.53−7.48 (m, 1H), 6.93 (s, 1H), 6.76 (s, 1H), 3.67 (s, 2H), 1.36 (s, 6H), 1.25 (s, 9H). ^{13}C NMR (126 MHz, $CDCl_3$) δ 162.7, 160.4, 158.3, 156.1, 146.3, 136.2, 125.5, 123.4, 105.6, 70.8, 56.3, 32.5, 30.4 (3C), 24.9 (2C). HRMS (ESI): calcd for $C_{17}H_{23}FN_4NaO_2$ $[M + Na]^+$, 357.1703; found 357.1670. mp: 117−119 °C. HPLC purity = 99.2%; t_R = 3.3 min.

*5-(tert-Butyl)-1-(5-chloropyridin-2-yl)-N-(1-hydroxy-2-methylpropan-2-yl)-1H-pyrazole-3-carboxamide (**65**).* The title compound was prepared by the same procedure described for **54** except using 5-chloro-2-hydrazinylpyridine hydrochloride instead of phenylhydrazine hydrochloride as a white solid. ^{1}H NMR (500 MHz, DMSO-d_6) δ 8.40 (s, 1H), 8.07 (d, J = 8.7 Hz, 1H), 7.96 (s, 1H), 7.72 (d, J = 8.7 Hz, 1H),

https://dx.doi.org/10.1021/acs.jmedchem.0c01023
J. Med. Chem. 2021, 64, 385−403

6.65 (s, 1H), 4.71 (t, J = 6.0 Hz, 1H), 3.44 (d, J = 6.0 Hz, 2H), 1.30 (s, 9H), 1.25 (s, 6H). ^{13}C NMR (126 MHz, $CDCl_3$) δ 163.3, 161.4, 150.5, 145.2, 139.4, 138.9, 129.8, 117.8, 108.8, 69.1, 56.7, 32.4, 30.1 (3C), 24.5 (2C). HRMS (ESI): calcd for $C_{17}H_{23}ClN_4NaO_2$ $[M + Na]^+$, 373.1407; found 373.1404. mp: 156−158 °C. HPLC purity = 96.1%; t_R = 4.5 min.

*5-(tert-Butyl)-N-(1-hydroxy-2-methylpropan-2-yl)-1-(5-(trifluoromethyl)pyridin-2-yl)-1H-pyrazole-3-carboxamide (**66**).* The title compound was prepared by the same procedure described for **54** except using 2-hydrazinyl-5-(trifluoromethyl)pyridine hydrochloride instead of phenylhydrazine hydrochloride as a white solid. ^{1}H NMR (400 MHz, $CDCl_3$) δ 8.84 (s, 1H), 8.13 (d, J = 8.3 Hz, 1H), 7.74 (d, J = 8.4 Hz, 1H), 6.92 (s, 1H), 6.81 (s, 1H), 4.93 (s, 1H), 3.68 (s, 2H), 1.37 (s, 6H), 1.33 (s, 9H). ^{13}C NMR (101 MHz, $CDCl_3$) δ 162.4, 156.6, 147.1, 145.1, 136.0, 126.6, 124.5, 121.7, 121.0, 106.7, 70.6, 56.3, 32.8, 30.4 (3C), 24.8 (2C). HRMS (ESI): calcd for $C_{18}H_{23}F_3N_4NaO_2$ $[M + Na]^+$, 407.1671; found 407.1640. mp: 136−138 °C. HPLC purity = 97.6%; t_R = 5.9 min.

*5-(tert-Butyl)-N-(1-hydroxy-2-methylpropan-2-yl)-1-(3-chloro-5-(trifluoromethyl)pyridin-2-yl)-1H-pyrazole-3-carboxamide (**67**).* The title compound was prepared by the same procedure described for **54** except using 2-hydrazinyl-3- chloro -5-(trifluoromethyl)pyridine hydrochloride instead of phenylhydrazine hydrochloride as a white solid. ^{1}H NMR (500 MHz, $CDCl_3$) δ 8.80 (s, 1H), 8.19 (s, 1H), 6.87 (s, 1H), 6.79 (s, 1H), 3.68 (s, 2H), 1.35 (s, 6H), 1.21 (s, 9H). ^{13}C NMR (126 MHz, DMSO-d_6) δ 160.8, 155.7, 153.4, 148.4, 144.8, 138.7, 130.8, 123.8, 121.7, 104.9, 68.4, 54.6, 32.2, 30.1 (3C), 23.6 (2C). HRMS (ESI): calcd for $C_{18}H_{23}ClF_3N_4O_2$ $[M + H]^+$, 419.1462; found 419.1460. mp: 199−201 °C. HPLC purity = 97.8%; t_R = 8.5 min.

*5-(tert-Butyl)-N-(1-hydroxy-2-methylpropan-2-yl)-1-(pyrimidin-2-yl)-1H-pyrazole-3-carboxamide (**68**).* The title compound was prepared by the same procedure described for **54** except using 2-hydrazinylpyrimidine hydrochloride instead of phenylhydrazine hydrochloride as a white solid. ^{1}H NMR (500 MHz, $CDCl_3$) δ 8.95−8.88 (m, 2H), 7.50−7.44 (m, 1H), 7.04 (s, 1H), 6.79 (s, 1H), 3.66 (s, 2H), 1.36 (s, 6H), 1.29 (s, 9H). ^{13}C NMR (126 MHz, DMSO-d_6) δ 161.1, 160.0 (2C), 158.8, 155.2, 147.3, 122.8, 104.9, 68.5, 54.6, 32.4, 30.5 (3C), 23.7 (2C). HRMS (ESI): calcd for $C_{16}H_{24}N_5O_2$ $[M + H]^+$, 318.1930; found 318.1927. mp: 111−113 °C. HPLC purity = 97.4%; t_R = 7.9 min.

Calcium Mobilization Assay. Calcium mobilization assays were performed as previously described,[57] and the EC_{50} or IC_{50} values were calculated using GraphPad Prism 7 software (GraphPad).

cAMP HTRF Assay. cAMP HTRF assays were performed using a Cisbio HTRF dynamic 2 cAMP kit (Gif-sur-Yvette, France) according to the manufacturer's instructions.[50] HEK293-CB2 cells were resuspended in HBSS buffer (containing 10 mM HEPES, 500 μM 3-isobutyl-1-methylxanthine) with a final cell density of 1×10^6 cells/mL. Cell suspension (5 μL, 5000 cells/well) loaded into shallow 384-well plates was mixed with 5 μL of cAMP assay buffer containing the indicated concentrations of compounds and forskolin (3 μM) for 15 min at rt. Then, detection buffer consisting of cAMP-d2 (5 μL) and anti-cAMP-cryptate (5 μL) was added to terminate the reaction. Upon 2 h incubation at rt away from light, HTRF signals were recorded using a Cytation 5 Imaging Reader (BioTek, Winooski, Vermont).

β-Arrestin Recruitment Assay. HEK293 cells were transfected with CB1/CB2-tTA fusion expression vector, a β-arrestin2-TEV fusion gene, and a tTA-dependent luciferase reporter using Lipofectamine 2000. Then, the transfected cells were seeded into 96-well white clear-bottom cell culture plates with a density of 25 000 cells per well. After 24 h, 20 μL of designed drug solutions was prepared and added to each well. Next day, luciferase activities were determined by adding Bright-Glo solution (Promega) and detected with a Cytation 5 Imaging Reader (BioTek, Winooski, Vermont). GraphPad Prism was used for data analysis.

ERK1/2 Phosphorylation Assay. Cells were starved with serum-free medium for 2 h and treated with indicated compounds for 15 min. Then, the treated cells were washed and harvested in RIPA lysis buffer with protease and phosphatase inhibitors (Roche; San Francisco, CA). Western blotting was conducted as previously described.[28,58] The primary anti-ERK1/2 antibody (1:1000; Cell Signaling Technology), anti-phospho-ERK1/2 antibody (Thr202/Tyr204) (1:1000; Cell Signaling Technology), and anti-GAPDH (1:10000; Sigma-Aldrich) were used.

Human Liver Microsome Assay. Human liver microsome assay was conducted by Wuxi AppTec Co. Ltd. The microsomes (Cat No. 452117) (0.5 mg/mL) were preincubated in 100 mM potassium phosphate buffer (pH = 7.4) with 1 μM tested compounds, 1 μM NADPH, and 10 mM $MgCl_2$ for 5 min at 37 °C. The reactions were initiated by the addition of 1 mM NADPH. After 0, 5, 10, 30, and 60 min incubations at 37 °C, the mixtures were quenched by adding cold CH_3CN with internal standard. Then, the samples were centrifuged at 4000 rpm for 20 min under 4 °C. Supernatants were used for analysis using a developed LC-MS/MS method.

PK Study. 18 BALB/c female mice, weighing between 20 and 24 g, were randomly divided into two groups. Compound **66** was intravenously or orally injected at 1 or 5 mg/kg. Plasma samples were collected at the following time points: 0.083, 0.25, 0.5, 1, 2, 4, 8, and 24 h upon administration (n = 3/group). Biological data collection and analysis of **66** were performed by a developed LC-MS/MS method. The PK parameters were then calculated using a nonatrioventricular model (Phoenix WinNonlin 7.0, Pharsight).

BLM-Induced SSc Model. The BLM-induced SSc model was developed as previously described.[28,50] Briefly, female Balb/c mice (6−8 weeks old) were obtained from the Experimental Animal Centre of the East China Normal University (ECNU) and fed in a sterile environment at 20 °C with a 12 h light/dark cycle. All of the animal experiments were approved by the Animal Experiments Committee of the ECNU(AR2013/06002). BLM in phosphate-buffered saline (PBS, 100 μL, 1 mg/mL) was subcutaneously injected in the shaved upper back of the mice once daily for 2 weeks. The mice were next randomly divided into five groups including negative controls (PBS only), BLM plus vehicle (BLM + PBS), BLM plus **9** (BLM + **9**), and BLM plus **66** (BLM + **66**, 1 or 5 mg/kg). Compounds **66** and **9** were dissolved in PBS with 0.3% Tween 80 and 0.1% DMSO, and subcutaneously injected in the shaved upper back once daily for 4 weeks. Finally, the mice were euthanized using CO_2 asphyxiation and the treated skin was extracted for further histological analysis.

RNA Isolation and Quantitative Real-Time PCR Assay. The total RNA of the mouse skin was isolated using RNAiso Plus (TaKaRa Biotechnology, Dalian, China). Reverse-transcription PCR was next performed using PrimeScript RT Master Mix (TaKaRa Biotechnology, Dalian, China). Quantitative real-time PCR (QPCR) analysis was performed using Applied Biosystems QuantStudio 3 Real-Time PCR Systems (Applied Biosystems, Rotkreuz, Switzerland). QPCR primers are listed in Table S1.

Docking Stimulations. Molecular docking studies between compound **40**, **66**, and CB2 receptor were performed using Schrödinger Glide software.[59] The X-ray crystal structure of human CB2 co-crystallized with antagonist AM10257 (PDB code: 5ZTY)[53] and Cryo-EM structure of human CB2-G_i protein in complex with agonist WIN 55,212−2 (PDB code: 6PT0)[52] were downloaded from the Protein Data Bank. The co-crystallized ligands were used to help define the active sites for docking studies. LigPrep was used to prepare high-quality,[60] all-atom three-dimensional (3D) structures of compounds **40** and **66**. Receptor grids were generated using Receptor Grid Generation in the Glide application of Maestro, and ligands were docked to the CB2 receptor using Glide version 5.8 docking protocol. The docking conformations with the lowest binding energy were selected for further analysis.

Statistical Data Analysis. Data were shown as mean ± SD. Datasets consisting of more than two groups were assessed using one-way ANOVA followed by Tukey's multiple comparison test. Statistical comparisons between two groups were analyzed using a two-tailed Student's t-test. Dose−response curve fitting and all of the statistical analyses were performed using GraphPad Prism 7 software (GraphPad). Statistical significance was defined as $^*P < 0.05$, $^{**}P < 0.01$, and $^{***}P < 0.001$.

https://dx.doi.org/10.1021/acs.jmedchem.0c01023
J. Med. Chem. 2021, 64, 385−403

■ ASSOCIATED CONTENT

Supporting Information

The Supporting Information is available free of charge at https://pubs.acs.org/doi/10.1021/acs.jmedchem.0c01023.

CB2 receptor antagonist AM630 inhibit calcium mobilization induced by **66**; primer sequences of QPCR; and characterization of key intermediates by 2D HMBC and ^{1}H NMR experiments (PDF)

Molecular formula strings (CSV)

■ AUTHOR INFORMATION

Corresponding Authors

Li-Fang Yu − *Shanghai Engineering Research Center of Molecular Therapeutics and New Drug Development, School of Chemistry and Molecular Engineering, East China Normal University, Shanghai 200062, P. R. China;* orcid.org/0000-0002-3250-6773; Email: lfyu@sat.ecnu.edu.cn

Weiqiang Lu − *Drug Discovery Unit, Shanghai Key Laboratory of Regulatory Biology, Institute of Biomedical Sciences and School of Life Sciences, East China Normal University, Shanghai 200241, P. R. China;* orcid.org/0000-0003-1349-6597; Email: wqlu@bio.ecnu.edu.cn

Han-Kun Zhang − *Drug Discovery Unit, Shanghai Key Laboratory of Regulatory Biology, Institute of Biomedical Sciences and School of Life Sciences, East China Normal University, Shanghai 200241, P. R. China;* orcid.org/0000-0002-5008-0825; Email: hkzhang@bio.ecnu.edu.cn

Authors

Bei-Er Jiang − *Drug Discovery Unit, Shanghai Key Laboratory of Regulatory Biology, Institute of Biomedical Sciences and School of Life Sciences, East China Normal University, Shanghai 200241, P. R. China; Navy Medical Research Institute, Second Military Medical University, Shanghai 200433, P. R. China*

Xingwu Jiang − *Drug Discovery Unit, Shanghai Key Laboratory of Regulatory Biology, Institute of Biomedical Sciences and School of Life Sciences, East China Normal University, Shanghai 200241, P. R. China; Department of Materials Science, Fudan University, Shanghai 200433, P. R. China*

Qiansen Zhang − *Drug Discovery Unit, Shanghai Key Laboratory of Regulatory Biology, Institute of Biomedical Sciences and School of Life Sciences, East China Normal University, Shanghai 200241, P. R. China;* orcid.org/0000-0002-8608-3067

Qiuwen Liang − *Drug Discovery Unit, Shanghai Key Laboratory of Regulatory Biology, Institute of Biomedical Sciences and School of Life Sciences, East China Normal University, Shanghai 200241, P. R. China*

Zi-Liang Qiu − *Drug Discovery Unit, Shanghai Key Laboratory of Regulatory Biology, Institute of Biomedical Sciences and School of Life Sciences, East China Normal University, Shanghai 200241, P. R. China*

Xiang-Bai Sun − *Drug Discovery Unit, Shanghai Key Laboratory of Regulatory Biology, Institute of Biomedical Sciences and School of Life Sciences, East China Normal University, Shanghai 200241, P. R. China*

Jun-Jie Yang − *Drug Discovery Unit, Shanghai Key Laboratory of Regulatory Biology, Institute of Biomedical Sciences and School of Life Sciences, East China Normal University, Shanghai 200241, P. R. China;* orcid.org/0000-0003-3997-1851

Si Chen − *Drug Discovery Unit, Shanghai Key Laboratory of Regulatory Biology, Institute of Biomedical Sciences and School of Life Sciences, East China Normal University, Shanghai 200241, P. R. China*

Chunyang Yi − *Drug Discovery Unit, Shanghai Key Laboratory of Regulatory Biology, Institute of Biomedical Sciences and School of Life Sciences, East China Normal University, Shanghai 200241, P. R. China*

Xiaolei Chai − *Drug Discovery Unit, Shanghai Key Laboratory of Regulatory Biology, Institute of Biomedical Sciences and School of Life Sciences, East China Normal University, Shanghai 200241, P. R. China*

Mingyao Liu − *Drug Discovery Unit, Shanghai Key Laboratory of Regulatory Biology, Institute of Biomedical Sciences and School of Life Sciences, East China Normal University, Shanghai 200241, P. R. China;* orcid.org/0000-0001-7339-5048

Complete contact information is available at: https://pubs.acs.org/10.1021/acs.jmedchem.0c01023

Author Contributions

$^{\perp}$B.-E.J., X.J., and Q.Z. contributed equally to this work.

Notes

The authors declare no competing financial interest.

■ ACKNOWLEDGMENTS

The authors thank the National Key R&D Program of China (2018YFA0507001), the National Natural Science Foundation of China (82073706, 21977032, 81830083, and 81972828), the Shanghai Committee of Science and Technology (18431900100, 18431900500, and 19ZR1473500), the Innovation Program of Shanghai Municipal Education Commission (2017−01−07−00−05-E00011), the Shenzhen Municipal Government of China (KQTD2017081060226082), and the ECNU Multifunctional Platform for Innovation (011). In addition, they thank Dr. Stefan Siwko for his assistance in proofreading the manuscript.

■ ABBREVIATIONS

Δ^9-THC, (−)-*trans*-Δ^9-tetrahydrocannabinol; ECS, endocannabinoid system; SSc, systemic sclerosis; BLM, bleomycin; SAR, structure−activity relationship; PK, pharmacokinetic; *t*-BuOK, potassium *tert*-butoxide; rt, room temperature; AcOH, acetic acid; HATU, 2-(7-aza-1*H*-benzotriazole-1-yl)-1,1,3,3-tetramethyluronium hexafluoro; DIPEA, *N*,*N*-diisopropylethylamine; NBS, *N*,*N*-diisopropylethylamine; NCS, *N*-chlorosuccinimide; TFAA, trifluoroacetic anhydride; cAMP, cyclic adenosine monophosphate; ERK, extracellular signal-regulated kinase; EGF, epidermal growth factor; α-SMA, α-smooth muscle actin; mp, melting point

■ REFERENCES

(1) Pertwee, R. G. Cannabinoid pharmacology: the first 66 years. *Br. J. Pharmacol.* **2006**, *147*, S163−S171.

(2) Pertwee, R. G. The pharmacology of cannabinoid receptors and their ligands: an overview. *Int. J. Obes.* **2006**, *30*, S13−S18.

(3) Gaoni, Y.; Mechoulam, R. Isolation, structure, and partial synthesis of an active constituent of hashish. *J. Am. Chem. Soc.* **1964**, *86*, 1646−1647.

(4) De Petrocellis, L.; Di Marzo, V. An introduction to the endocannabinoid system: from the early to the latest concepts. *Best Pract. Res., Clin. Endocrinol. Metab.* **2009**, *23*, 1−15.

(5) Brindisi, M.; Maramai, S.; Gemma, S.; Brogi, S.; Grillo, A.; Mannelli, L. D. C.; Gabellieri, E.; Lamponi, S.; Saponara, S.; Gorelli, B.; et al. Development and pharmacological characterization of selective blockers of 2-arachidonoyl glycerol degradation with efficacy in rodent models of multiple sclerosis and pain. *J. Med. Chem.* **2016**, *59*, 2612−2632.
(6) Pertwee, R. G.; Howlett, A. C.; Abood, M. E.; Alexander, S. P. H.; Marzo, V. D.; Elphick, M. R.; Greasley, P. J.; Hansen, H. S.; Kunos, G.; Mackie, K.; et al. International union of basic and clinical pharmacology. LXXIX. Cannabinoid receptors and their ligands: Beyond CB1 and CB2. *Pharmacol. Rev.* **2010**, *62*, 588−631.
(7) Panagis, G.; Mackey, B.; Vlachou, S. Cannabinoid regulation of brain reward processing with an emphasis on the role of CB1 receptors: a step back into the future. *Front. Psychiatry* **2014**, *5*, 92.
(8) Farquhar-Smith, W. P.; Egertova, M.; Bradbury, E. J.; McMahon, S. B.; Rice, A. S.; Elphick, M. R. Cannabinoid CB(1) receptor expression in rat spinal cord. *Mol. Cell. Neurosci.* **2000**, *15*, 510−521.
(9) Blasio, A.; Iemolo, A.; Sabino, V.; Petrosino, S.; Steardo, L.; Rice, K. C.; Orlando, P.; Iannotti, F. A.; Di Marzo, V.; Zorrilla, E. P.; Cottone, P. Rimonabant precipitates anxiety in rats withdrawn from palatable food: role of the central amygdala. *Neuropsychopharmacology* **2013**, *38*, 2498−2507.
(10) Jones, D. End of the line for cannabinoid receptor 1 as an anti-obesity target? *Nat. Rev. Drug Discovery* **2008**, *7*, 961−962.
(11) Després, J.-P.; Golay, A.; Sjostrom, L. Rimonabant in Obesity-Lipids Study, G. Effects of rimonabant on metabolic risk factors in overweight patients with dyslipidemia. *N. Engl. J. Med.* **2005**, *353*, 2121−2134.
(12) Hollinshead, S. P.; Tidwell, M. W.; Palmer, J.; Guidetti, R.; Sanderson, A.; Johnson, M. P.; Chambers, M. G.; Oskins, J.; Stratford, R.; Astles, P. C. Selective cannabinoid receptor type 2 (CB2) agonists: optimization of a series of purines leading to the identification of a clinical candidate for the treatment of osteoarthritic pain. *J. Med. Chem.* **2013**, *56*, 5722−5733.
(13) Cheng, Y.; Hitchcock, S. A. Targeting cannabinoid agonists for inflammatory and neuropathic pain. *Expert Opin. Invest. Drugs* **2007**, *16*, 951−965.
(14) Benito, C.; Romero, J. P.; Tolón, R. M.; Clemente, D.; Docagne, F.; Hillard, C. J.; Guaza, C.; Romero, J. Cannabinoid CB1 and CB2 receptors and fatty acid amide hydrolase are specific markers of plaque cell subtypes in human multiple sclerosis. *J. Neurosci.* **2007**, *27*, 2396−2402.
(15) Cassano, T.; Calcagnini, S.; Pace, L.; De Marco, F.; Romano, A.; Gaetani, S. Cannabinoid receptor 2 signaling in neurodegenerative disorders: from pathogenesis to a promising therapeutic target. *Front. Neurosci.* **2017**, *11*, 30.
(16) Sarfaraz, S.; Afaq, F.; Adhami, V. M.; Mukhtar, H. Cannabinoid receptor as a novel target for the treatment of prostate cancer. *Cancer Res.* **2005**, *65*, 1635−1641.
(17) Idris, A. I. Cannabinoid receptors as target for treatment of osteoporosis: a tale of two therapies. *Curr. Neuropharmacol.* **2010**, *8*, 243−253.
(18) McKallip, R. J.; Lombard, C.; Fisher, M.; Martin, B. R.; Ryu, S.; Grant, S.; Nagarkatti, P. S.; Nagarkatti, M. Targeting CB2 cannabinoid receptors as a novel therapy to treat malignant lymphoblastic disease. *Blood* **2002**, *100*, 627−634.
(19) Thakur, G. A.; Tichkule, R.; Bajaj, S.; Makriyannis, A. Latest advances in cannabinoid receptor agonists. *Expert Opin. Ther. Pat.* **2009**, *19*, 1647−1673.
(20) Ostenfeld, T.; Price, J.; Albanese, M.; Bullman, J.; Guillard, F.; Meyer, I.; Leeson, R.; Costantin, C.; Ziviani, L.; Nocini, P. F.; Milleri, S. A randomized, controlled study to investigate the analgesic efficacy of single doses of the cannabinoid receptor-2 agonist GW842166, ibuprofen or placebo in patients with acute pain following third molar tooth extraction. *Clin. J. Pain* **2011**, *27*, 668−676.
(21) https://clinicaltrials.gov/ct2/show/NCT01319929 (accessed Sep 20, 2019).
(22) https://clinicaltrials.gov/ct2/show/NCT00697710 (accessed Sep 20, 2019).
(23) https://www.corbuspharma.com/ (accessed Sep 25, 2019).
(24) Beyer, C.; Schett, G.; Distler, O.; Distler, J. H. W. Animal models of systemic sclerosis: Prospects and limitations. *Arthritis Rheum.* **2010**, *62*, 2831−2844.
(25) Varga, J.; Abraham, D. Systemic sclerosis: a prototypic multisystem fibrotic disorder. *J. Clin. Invest.* **2007**, *117*, 557−567.
(26) Yazawa, N.; Fujimoto, M.; Tamaki, K. Recent advances on pathogenesis and therapies in systemic sclerosis. *Clin. Rev. Allergy. Immunol.* **2007**, *33*, 107−112.
(27) Denton, C. P. Advances in pathogenesis and treatment of systemic sclerosis. *Clin. Med.* **2015**, *15*, s58−s63.
(28) Gonzalez, E. G.; Selvi, E.; Balistreri, E.; Akhmetshina, A.; Palumbo, K.; Lorenzini, S.; Lazzerini, P. E.; Montilli, C.; Capecchi, P. L.; Lucattelli, M.; Baldi, C.; Gianchecchi, E.; Galeazzi, M.; Pasini, F. L.; Distler, J. H. Synthetic cannabinoid ajulemic acid exerts potent antifibrotic effects in experimental models of systemic sclerosis. *Ann. Rheum. Dis.* **2012**, *71*, 1545−1551.
(29) Akhmetshina, A.; Dees, C.; Busch, N.; Beer, J.; Sarter, K.; Zwerina, J.; Zimmer, A.; Distler, O.; Schett, G.; Distler, J. H. The cannabinoid receptor CB2 exerts antifibrotic effects in experimental dermal fibrosis. *Arthritis Rheum.* **2009**, *60*, 1129−1136.
(30) Balistreri, E.; Garcia-Gonzalez, E.; Selvi, E.; Akhmetshina, A.; Palumbo, K.; Lorenzini, S.; Maggio, R.; Lucattelli, M.; Galeazzi, M.; Distler, J. W. The cannabinoid WIN55, 212-2 abrogates dermal fibrosis in scleroderma bleomycin model. *Ann. Rheum. Dis.* **2011**, *70*, 695−699.
(31) https://www.americanpharmaceuticalreview.com/1315-News/175177-FDA-Designates-Corbus-Pharmaceuticals-Resunab-an-Orphan-Drug/ (accessed Sep 30, 2019).
(32) Banister, S. D.; Wilkinson, S. M.; Longworth, M.; Stuart, J.; Apetz, N.; English, K.; Brooker, L.; Goebel, C.; Hibbs, D. E.; Glass, M.; et al. The synthesis and pharmacological evaluation of adamantane-derived indoles: cannabimimetic drugs of abuse. *ACS Chem. Neurosci.* **2013**, *4*, 1081−1092.
(33) Martinotti, G.; Santacroce, R.; Papanti, D.; Elgharably, Y.; Prilutskaya, M.; Corazza, O. Synthetic cannabinoids: psychopharmacology, clinical aspects, psychotic onset. *CNS Neurol. Disord.: Drug Targets* **2017**, *16*, 567−575.
(34) Tai, S.; Fantegrossi, W. E. Pharmacological and toxicological effects of synthetic cannabinoids and their metabolites. In *Neuropharmacology of New Psychoactive Substances (NPS)*; Current Topics in Behavioral Neurosciences; Springer: Cham, 2016; Vol. *32*, pp 249−262.
(35) Basavarajappa, B. S.; Subbanna, S. Potential mechanisms underlying the deleterious effects of synthetic cannabinoids found in spice/K2 products. *Brain Sci.* **2019**, *9*, 14.
(36) Banister, S. D.; Stuart, J.; Kevin, R. C.; Edington, A.; Longworth, M.; Wilkinson, S. M.; Beinat, C.; Buchanan, A. S.; Hibbs, D. E.; Glass, M.; Connor, M.; McGregor, I. S.; Kassiou, M. Effects of bioisosteric fluorine in synthetic cannabinoid designer drugs JWH-018, AM-2201, UR-144, XLR-11, PB-22, 5F-PB-22, APICA, and STS-135. *ACS Chem. Neurosci.* **2015**, *6*, 1445−1458.
(37) Banister, S. D.; Moir, M.; Stuart, J.; Kevin, R. C.; Wood, K. E.; Longworth, M.; Wilkinson, S. M.; Beinat, C.; Buchanan, A. S.; Glass, M.; Connor, M.; McGregor, I. S.; Kassiou, M. Pharmacology of indole and indazole synthetic cannabinoid designer drugs AB-FUBINACA, ADB-FUBINACA, AB-PINACA, ADB-PINACA, 5F-AB-PINACA, 5F-ADB-PINACA, ADBICA, and 5F-ADBICA. *ACS Chem. Neurosci.* **2015**, *6*, 1546−1559.
(38) Banister, S. D.; Longworth, M.; Kevin, R.; Sachdev, S.; Santiago, M.; Stuart, J.; Mack, J. B.; Glass, M.; McGregor, I. S.; Connor, M.; Kassiou, M. Pharmacology of valinate and tert-leucinate synthetic cannabinoids 5F-AMBICA, 5F-AMB, 5F-ADB, AMB-FUBINACA, MDMB-FUBINACA, MDMB-CHMICA, and their analogues. *ACS Chem. Neurosci.* **2016**, *7*, 1241−1254.
(39) Longworth, M.; Connor, M.; Banister, S. D.; Kassiou, M. Synthesis and pharmacological profiling of the metabolites of synthetic cannabinoid drugs APICA, STS-135, ADB-PINACA, and 5F-ADB-PINACA. *ACS Chem. Neurosci.* **2017**, *8*, 1673−1680.

(40) Shi, Y.; Duan, Y. H.; Ji, Y. Y.; Wang, Z. L.; Wu, Y. R.; Gunosewoyo, H.; Xie, X. Y.; Chen, J. Z.; Yang, F.; Li, J.; Tang, J.; Xie, X.; Yu, L. F. Amidoalkylindoles as potent and selective cannabinoid type 2 receptor agonists with in vivo efficacy in a mouse model of multiple sclerosis. *J. Med. Chem.* **2017**, *60*, 7067−7083.
(41) Moir, M.; Lane, S.; Lai, F.; Connor, M.; Hibbs, D. E.; Kassiou, M. Strategies to develop selective CB2 receptor agonists from indole carboxamide synthetic cannabinoids. *Eur. J. Med. Chem.* **2019**, *180*, 291−309.
(42) Kevin, R. C.; Lefever, T. W.; Snyder, R. W.; Patel, P. R.; Fennell, T. R.; Wiley, J. L.; McGregor, I. S.; Thomas, B. F. In vitro and in vivo pharmacokinetics and metabolism of synthetic cannabinoids CUMYL-PICA and 5F-CUMYL-PICA. *Forensic Toxicol.* **2017**, *35*, 333−347.
(43) Sobolevsky, T.; Prasolov, I.; Rodchenkov, G. Study on the phase I metabolism of novel synthetic cannabinoids, APICA and its fluorinated analogue. *Drug Test. Anal.* **2015**, *7*, 131−142.
(44) Gatley, S. J.; Lan, R.; Volkow, N. D.; Pappas, N.; King, P.; Wong, C. T.; Gifford, A. N.; Pyatt, B.; Dewey, S. L.; Makriyannis, A. Imaging the brain marijuana receptor: development of a radioligand that binds to cannabinoid CB1 receptors in vivo. *J. Neurochem.* **1998**, *70*, 417−423.
(45) Francisco, M. E.; Seltzman, H. H.; Gilliam, A. F.; Mitchell, R. A.; Rider, S. L.; Pertwee, R. G.; Stevenson, L. A.; Thomas, B. F. Synthesis and structure-activity relationships of amide and hydrazide analogues of the cannabinoid CB(1) receptor antagonist N-(piperidinyl)- 5-(4-chlorophenyl)-1-(2,4-dichlorophenyl)-4-methyl-1H-pyrazole-3-carboxamide (SR141716). *J. Med. Chem.* **2002**, *45*, 2708−2719.
(46) Szabo, G.; Varga, B.; Payer-Lengyel, D.; Szemzo, A.; Erdelyi, P.; Vukics, K.; Szikra, J.; Hegyi, E.; Vastag, M.; Kiss, B.; Laszy, J.; Gyertyan, I.; Fischer, J. Chemical and biological investigation of cyclopropyl containing diaryl-pyrazole-3-carboxamides as novel and potent cannabinoid type 1 receptor antagonists. *J. Med. Chem.* **2009**, *52*, 4329−4337.
(47) Donohue, S. R.; Dannals, R. F.; Halldin, C.; Pike, V. W. N-(4-cyanotetrahydro-2H-pyran-4-yl) and N-(1-cyanocyclohexyl) derivatives of 1,5-diarylpyrazole-3-carboxamides showing high affinity for 18 kDa translocator protein and/or cannabinoid receptors. *J. Med. Chem.* **2011**, *54*, 2961−2970.
(48) Hwang, S. H.; Wagner, K. M.; Morisseau, C.; Liu, J. Y.; Dong, H.; Wecksler, A. T.; Hammock, B. D. Synthesis and structure-activity relationship studies of urea-containing pyrazoles as dual inhibitors of cyclooxygenase-2 and soluble epoxide hydrolase. *J. Med. Chem.* **2011**, *54*, 3037−3050.
(49) Tyagarajan, S.; Chakravarty, P. K.; Zhou, B.; Taylor, B.; Fisher, M. H.; Wyvratt, M. J.; Lyons, K.; Klatt, T.; Li, X.; Kumar, S.; Williams, B.; Felix, J.; Priest, B. T.; Brochu, R. M.; Warren, V.; Smith, M.; Garcia, M.; Kaczorowski, G. J.; Martin, W. J.; Abbadie, C.; McGowan, E.; Jochnowitz, N.; Parsons, W. H. Substituted biaryl pyrazoles as sodium channel blockers. *Bioorg. Med. Chem. Lett.* **2010**, *20*, 5480−5483.
(50) Jiang, X.; Chen, S.; Zhang, Q.; Yi, C.; He, J.; Ye, X.; Liu, M.; Lu, W. Celastrol is a novel selective agonist of cannabinoid receptor 2 with anti-inflammatory and anti-fibrotic activity in a mouse model of systemic sclerosis. *Phytomedicine* **2020**, *67*, 153160.
(51) Pennington, L. D.; Moustakas, D. T. The Necessary nitrogen atom: a versatile high-impact design element for multiparameter optimization. *J. Med. Chem.* **2017**, *60*, 3552−3579.
(52) Xing, C.; Zhuang, Y.; Xu, T. H.; Feng, Z.; Zhou, X. E.; Chen, M.; Wang, L.; Meng, X.; Xue, Y.; Wang, J.; Liu, H.; McGuire, T. F.; Zhao, G.; Melcher, K.; Zhang, C.; Xu, H. E.; Xie, X. Q. Cryo-EM structure of the human cannabinoid receptor CB2-Gi signaling complex. *Cell* **2020**, *180*, 645−654.
(53) Li, X.; Hua, T.; Vemuri, K.; Ho, J. H.; Wu, Y.; Wu, L.; Popov, P.; Benchama, O.; Zvonok, N.; Locke, K.; Qu, L.; Han, G. W.; Iyer, M. R.; Cinar, R.; Coffey, N. J.; Wang, J.; Wu, M.; Katritch, V.; Zhao, S.; Kunos, G.; Bohn, L. M.; Makriyannis, A.; Stevens, R. C.; Liu, Z. J. Crystal structure of the human cannabinoid receptor CB2. *Cell* **2019**, *176*, 459−467.
(54) Dobovišek, L.; Hojnik, M.; Ferk, P. Overlapping molecular pathways between cannabinoid receptors type 1 and 2 and estrogens/androgens on the periphery and their involvement in the pathogenesis of common diseases (Review). *Int. J. Mol. Med.* **2016**, *38*, 1642−1651.
(55) Wetter, J. A.; Revankar, C.; Hanson, B. J. Utilization of the Tango beta-arrestin recruitment technology for cell-based EDG receptor assay development and interrogation. *J. Biomol. Screening* **2009**, *14*, 1134−1141.
(56) Rajagopal, S.; Shenoy, S. K. GPCR desensitization: Acute and prolonged phases. *Cell Signalling* **2018**, *41*, 9−16.
(57) Jiang, X. W.; Jiang, B. E.; Liu, H.; Liu, Z. T.; Hu, L. L.; Liu, M.; Lu, W.; Zhang, H. K. Design, synthesis, and biological evaluations of phenylpropiolic acid derivatives as novel GPR40 agonists. *Eur. J. Med. Chem.* **2018**, *158*, 123−133.
(58) Jiang, X.; Lu, W.; Shen, X.; Wang, Q.; Lv, J.; Liu, M.; Cheng, F.; Zhao, Z.; Pang, X. Repurposing sertraline sensitizes non-small cell lung cancer cells to erlotinib by inducing autophagy. *JCI Insight* **2018**, *3*, No. e98921.
(59) Friesner, R. A.; Banks, J. L.; Murphy, R. B.; Halgren, T. A.; Klicic, J. J.; Mainz, D. T.; Repasky, M. P.; Knoll, E. H.; Shelley, M.; Perry, J. K.; Shaw, D. E.; Francis, P.; Shenkin, P. S. Glide: a new approach for rapid, accurate docking and scoring. 1. Method and assessment of docking accuracy. *J. Med. Chem.* **2004**, *47*, 1739−1749.
(60) Greenwood, J. R.; Calkins, D.; Sullivan, A. P.; Shelley, J. C. Towards the comprehensive, rapid, and accurate prediction of the favorable tautomeric states of drug-like molecules in aqueous solution. *J. Comput.-Aided Mol. Des.* **2010**, *24*, 591−604.

https://dx.doi.org/10.1021/acs.jmedchem.0c01023
J. Med. Chem. 2021, 64, 385−403